

Dark Matter in the Coming Decade: Complementary Paths to Discovery and Beyond

Sebastian Arrenberg, University of Zürich; **Howard Baer**, University of Oklahoma; **Vernon Barger**, University of Wisconsin; **Laura Baudis**, University of Zürich; **Daniel Bauer**, Fermilab; **James Buckley**, Washington University; **Matthew Cahill-Rowley**, SLAC; **Randel Cotta**, University of California, Irvine; **Alex Drlica-Wagner**, SLAC; **Jonathan L. Feng**, University of California, Irvine; **Stefan Funk**, SLAC; **JoAnne Hewett**, SLAC; **Dan Hooper***, Fermilab; **Ahmed Ismail**, SLAC; **Manoj Kaplinghat***, University of California, Irvine; **Kyoungchul Kong**, University of Kansas; **Alexander Kusenko**, University of California, Los Angeles; **Konstantin Matchev***, University of Florida; **Mathew McCaskey**, University of Kansas; **Daniel McKinsey**, Yale University; **Dan Mickelson**, University of Oklahoma; **Tom Rizzo**, SLAC; **David Sanford**, Caltech; **Gabe Shaughnessy**, University of Wisconsin; **William Shepherd**, University of California, Santa Cruz; **Tim M. P. Tait***, University of California, Irvine; **Xerxes Tata**, University of Hawaii; **Sean Tulin**, University of Michigan; **Alexander M. Wijangco**, University of California, Irvine; **Matthew Wood**, SLAC; **Jonghee Yoo**, Fermilab; **Hai-Bo Yu**, University of California, Riverside;
on behalf of the Snowmass 2013 Cosmic Frontier WG4 "Dark Matter Complementarity"

Conveners: **Dan Hooper**, **Manoj Kaplinghat**, **Konstantin Matchev**

(Dated: 30 October 2013)

In this Report we discuss the four complementary searches for the identity of dark matter: direct detection experiments that look for dark matter interacting in the lab, indirect detection experiments that connect lab signals to dark matter in our own and other galaxies, collider experiments that elucidate the particle properties of dark matter, and astrophysical probes sensitive to non-gravitational interactions of dark matter. The complementarity among the different dark matter searches is discussed qualitatively and illustrated quantitatively in several theoretical scenarios. Our primary conclusion is that the diversity of possible dark matter candidates requires a balanced program based on all four of those approaches.

Contents

I. Introduction	2
II. Dark Matter Candidates	4
1. Neutralinos and other Supersymmetric WIMPs	5
2. Dark Matter from Extra Dimensions	5
3. Axions	5
4. Gravitinos	6
5. Asymmetric Dark Matter	6
6. Non-thermal WIMPs	6
7. Hidden Sector Dark Matter	7
III. The Four Pillars of Dark Matter Detection	7
A. Direct Detection	7

* Corresponding authors: dhooper@fnal.gov, mkapling@uci.edu, matchev@phys.ufl.edu, and ttait@uci.edu

1. Scattering of WIMPs on nuclei	7
2. Direct Axion Searches	8
B. Indirect Detection	8
C. Particle Colliders	9
D. Astrophysical Probes	10
IV. Qualitative Complementarity	12
V. Quantitative Complementarity	13
A. Effective Operator Description	13
B. Supersymmetry	15
1. The phenomenological MSSM (pMSSM)	15
2. Specific MSSM scenarios	17
3. The Next-to-minimal MSSM (NMSSM)	21
C. Universal Extra Dimensions	23
D. Self-interacting dark matter	26
VI. Post-Discovery Complementarity	30
VII. Conclusions	31
References	31

I. INTRODUCTION

Despite being five times as abundant as normal matter in the Universe, the identity of dark matter is unknown. Its existence, however, implies that our inventory of the basic building blocks of nature is incomplete, and uncertainty about its properties clouds attempts to fully understand how the Universe evolved to its present state and how it will evolve in the future. Uncovering the identity of dark matter is therefore a central and grand challenge for both fundamental physics and astronomy. Fortunately, a very promising array of groundbreaking experiments are positioned to transform the field of dark matter in the coming decade. The prospect that dark matter particles might be observed in the near future has drawn many new researchers to the field, which is now characterized by an extraordinary diversity of approaches unified by the common goal of discovering the identity of dark matter.

Dark matter was first postulated in its modern form in the 1930s to explain the anomalously large velocities of galaxies in the Coma cluster [1]. Over the subsequent decades, evidence for dark matter grew to include data from galactic rotation curves [2–4], and more recently from weak [5] and strong [6] lensing, hot gas in clusters [7, 8], the Bullet Cluster [9], Big Bang nucleosynthesis (BBN) [10], distant supernovae [11, 12], the statistical distribution of galaxies [13, 14] and the cosmic microwave background (CMB) [15, 16]. Together, these data provide an overwhelming body of evidence in support of the conclusion that cold (or possibly warm) dark matter makes up roughly a quarter of the total energy density of the Universe, exceeding the density of normal matter by about a factor of five.

Although these observations strongly support the existence of dark matter, they each do so uniquely through the dark matter’s gravitational influence on visible matter. As a consequence, these observations do little to shed light on the particle identity of dark matter, since all forms of matter interact universally through the force of gravity. If dark matter’s nature is to be understood, it is necessary that it be detected through non-gravitational interactions. Possibilities for such observations include the elastic scattering of dark matter with nuclei in a detector (direct detection), the detection of standard model particles produced in the annihilations or decays of dark matter (indirect detection), the production of dark matter particles at colliders, and the effects of dark matter interactions on astrophysical systems.

The prospects for each of these observational approaches, of course, depend considerably on the dark matter candidate under consideration, for which there are very many possibilities (for reviews, see, *e.g.*, Refs. [17–19]). In the case of weakly interacting massive particles (WIMPs), dark matter particles are expected to have been produced in the hot early Universe and then annihilate in pairs. Those that survive to the present are known as “thermal relics” [20–23]. The realization that a stable particle species with a GeV–TeV mass and an annihilation cross section near the scale of the weak interaction will yield a thermal relic abundance similar to the observed cosmological abundance of dark matter ($\Omega_X \sim \mathcal{O}(0.1)$) has provided a great deal of motivation for dark matter in the form of WIMPs. Furthermore, WIMPs are generically predicted in a wide variety of weak-scale extensions of the standard model, including models with supersymmetry [24, 25], extra spatial dimensions [26–29], and many others [30–32].

In addition to WIMPs, there are many other well motivated and often studied candidates for dark matter. Axions [33–36] are motivated by the fact that, despite observations to the contrary, the strong interaction of the standard model is naturally expected to induce significant CP violating effects. Although the Peccei-Quinn mechanism is capable of elegantly solving this problem, it also predicts the existence of a very light and extremely weakly interacting axion, which could make up the observed dark matter abundance. Right-handed or sterile neutrinos are motivated by the observation of non-zero neutrino masses, and for certain ranges of masses and interaction strengths, may also be viable candidates for dark matter [37–39]. Alternatively, dark matter may be in a so-called hidden sector, which has its own set of matter particles and forces through which the dark matter interacts with other currently unknown particles [40, 41]. Another possibility is that the dark matter may be asymmetric [42–46], with a slight imbalance between the numbers of dark particles and dark antiparticles in the early universe. These particles annihilate until only the slight excess of dark particles remains. In many models, the dark matter asymmetry is related to the baryon-antibaryon asymmetry, and one expects the number of dark matter particles in the Universe to be similar to the number of baryons. Since dark matter contributes roughly five times more to the energy density of the Universe than normal matter, this scenario predicts dark matter particles with a mass on the order of $\sim 1 - 15$ GeV.

Although these dark matter candidates differ in important ways, in most cases they have non-gravitational interactions through which they may be detected. The non-gravitational interactions may be with any of the known particles or, as noted above for hidden sector dark matter, with other currently unknown particles. These possibilities are illustrated in Fig. 1, where the particles are grouped into four categories: nuclear matter, leptons, photons and other bosons, and other as-yet unknown particles. Dark matter may interact with one type of particle, or it may interact with several.

As we will discuss, discovering the particle identity of dark matter will most likely require synergistic progress along many different lines of inquiry. Our primary conclusion is that the diversity of possible dark matter candidates, and the diversity of their observational and experimental signatures, motivates a broad and well-balanced program of research. In particular, such a program requires a diverse array of experiments, together covering each of what we will refer to as the four pillars of dark matter discovery:

- *Direct Detection.* Dark matter scatters off a detector, producing a detectable signal. Prime examples are the detection of WIMPs through scattering off nuclei and the detection of axions through their interaction with photons in a magnetic field.
- *Indirect Detection.* Pairs of dark matter particles annihilate producing high-energy particles (antimatter, neutrinos, or photons). Alternatively, dark matter may be metastable, and its decay may produce the same high-energy particles.
- *Particle Colliders.* Particle colliders, such as the Large Hadron Collider (LHC) and proposed

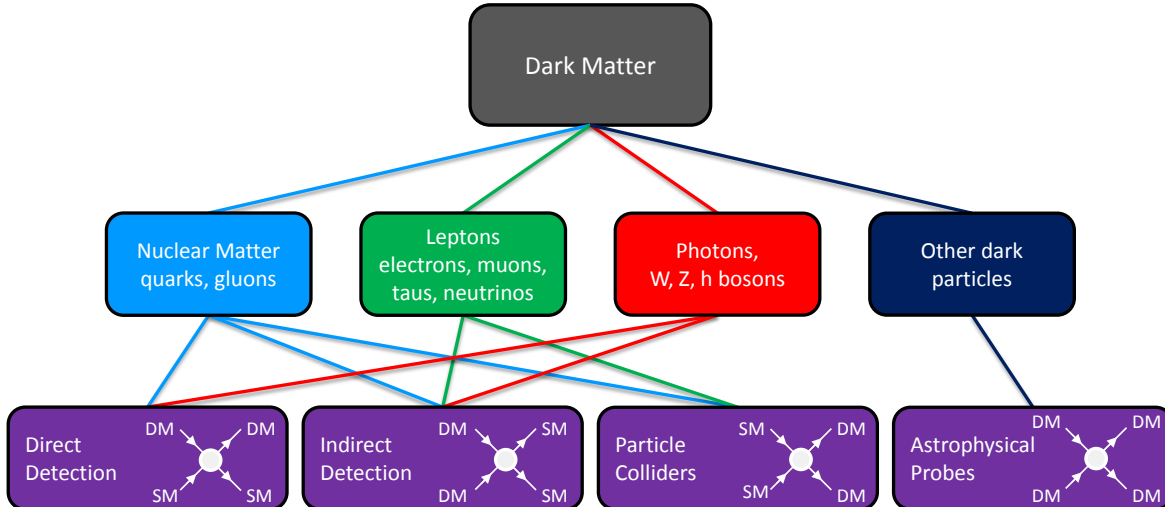


FIG. 1: Dark matter may have non-gravitational interactions with one or more of four categories of particles: nuclear matter, leptons, photons and other bosons, and other dark particles. These interactions may then be probed by four complementary approaches: direct detection, indirect detection, particle colliders, and astrophysical probes. The lines connect the experimental approaches with the categories of particles that they most stringently probe (additional lines can be drawn in specific model scenarios). The diagrams give example reactions of dark matter with standard model particles (SM) for each experimental approach.

future colliders, produce dark matter particles, which escape the detector, but are discovered as an excess of events with missing energy or momentum.

- *Astrophysical Probes.* The particle properties of dark matter are constrained through its impact on astrophysical observables. In particular, dark matter’s non-gravitational interactions could observably impact the densities of dark matter present in the central regions of galaxies, or the amount of dark matter substructure found in halos. Such interactions may also alter the cooling rates of stars, and influence the pattern of temperature fluctuations observed in the cosmic microwave background.

These search strategies are each shown in Fig. 1 and are connected to the particle interactions that they *most stringently* probe.

After summarizing many of the most promising particle candidates for dark matter in Sec. II, we return in Sec. III to these four pillars in more detail, discussing the current status and future prospects of direct, indirect, and collider searches for dark matter, as well as the impact of astrophysical observations. In Sec. IV we begin the discussion of the complementarity between different dark matter search strategies at a qualitative level. We extend this further in Sec. V, discussing quantitatively the interplay between experimental approaches, considering a number of representative particle physics frameworks. Finally, we summarize our conclusions in Sec. VII.

II. DARK MATTER CANDIDATES

In this section, we briefly summarize a number of specific dark matter candidates and candidate classes that have been considered in the literature. While certainly not exhaustive, this discussion is intended to reflect a representative sample of how the particle physics community currently views the form that dark matter particles might take.

1. Neutralinos and other Supersymmetric WIMPs

Models with weak-scale supersymmetry are motivated by a number of theoretically attractive features, including their ability to solve the electroweak hierarchy problem [47–50], allow for the high-scale unification of the standard model gauge couplings [51–55], and provide a viable candidate for the dark matter of our Universe [24, 25]. In particular, in models with unbroken R -parity, the lightest supersymmetric particle (LSP) is stable. If the LSP is a neutralino (a mixture of the superpartners of the neutral gauge and Higgs bosons), it will be a WIMP. Sneutrinos could also constitute a WIMP, although constraints from direct detection experiments exclude this possibility in minimal models. Gravitinos could also be the LSP, but in this case the dark matter would be far less than weakly interacting and would require a non-thermal origin in the early Universe (see below).

In recent years, null results from the LHC and direct detection experiments have begun to significantly constrain the parameter space of most commonly studied supersymmetric models. However, neutralino dark matter remains viable as a thermal relic in a number of regions of parameter space, including those in which its depletion in the early Universe occurs through coannihilations with another species (such as a stau or stop), or through the neutral heavy Higgs resonance. It is also possible that the LSP is a mixture of gauginos and higgsinos (*e.g.* focus point models), or is a relatively heavy wino ($m_\chi \approx 2.7\text{--}3\text{ TeV}$) or higgsino ($m_\chi \approx 1\text{ TeV}$).

2. Dark Matter from Extra Dimensions

If there exist dimensions of space beyond the three we directly experience, Kaluza-Klein (KK) excitations of standard model particles could potentially make up the dark matter of the universe. In models with one (or more) universal, flat dimension, KK parity (a remnant of n -dimensional momentum conservation) can stabilize the lightest KK state. Of particular interest is the lightest KK excitation of the hypercharge gauge boson [26, 27], which for a $\sim\text{TeV}$ scale mass leads to a thermal relic abundance similar to the observed dark matter abundance. KK dark matter candidates in other scenarios have also been proposed, including those arising in scenarios with warped extra dimensions [28, 56].

3. Axions

In the standard model, the naive expectation for the neutron’s electric dipole moment is roughly 10^{12} times larger than is allowed experimentally. It was recognized by Peccei and Quinn, however, that this “strong CP problem” could be solved by introducing a spontaneously broken global $U(1)$ symmetry which dynamically suppresses the CP violation induced by QCD [33]. The Goldstone boson of this broken global symmetry is the axion, which acquires a mass from the QCD anomaly [34, 35]. In light of experimental and astrophysical constraints, the scale of this symmetry breaking must be very high, implying that the axion will be very light ($m_a \lesssim 0.01\text{ eV}$) and extremely feebly interacting. Such particles never reach thermal equilibrium in the early Universe, but are predicted to be produced as cold dark matter through non-thermal mechanisms (such as through vacuum misalignment).

Efforts to probe the parameter space in which axions could constitute the dark matter of our Universe rely on the photon-photon-axion coupling [57]. In particular, microwave cavity experiments utilizing this interaction have begun to constrain a small fraction of such models, and are well-positioned to test the a much larger fraction of the axion dark matter window in the relatively near future.

4. Gravitinos

If the lightest supersymmetric particle is the superpartner of the graviton, it could also constitute the dark matter. Unlike the case of neutralinos or other WIMPs, the extremely feeble interactions of the gravitino prevent it from reaching thermal equilibrium with the thermal bath present in the early Universe. As a consequence, the surviving density of gravitinos depends strongly on the temperature to which the Universe was reheated following inflation.

The mass of the gravitino can be constrained by requiring that the decays of heavier superpartners do not destroy the successful predictions of big bang nucleosynthesis or overly alter the characteristics of the cosmic microwave background. If the gravitino is very light ($\lesssim 100$ MeV), however, the heavier superpartners will be sufficiently short lived as to decay prior to big bang nucleosynthesis, thus evading these constraints [58, 59]. Alternatively, if the gravitino mass is of the same order of magnitude as that of the next-to-lightest superpartner (presumably near the electroweak-scale), such decays can occur after the formation of light elements, but early enough to not unacceptably distort the cosmic microwave background. In this later case, the gravitino dark matter could originate from the decays of heavier superpartners, in what is known as the “superWIMP” scenario [60, 61].

5. Asymmetric Dark Matter

In asymmetric dark matter (ADM) scenarios, the dark matter relic abundance today is linked to a primordial dark asymmetry generated in the early Universe. The situation is analogous to how the baryon density arises: the Universe carries a net baryon number, such that when baryons and antibaryons annihilate around the QCD epoch, the residual asymmetric density of baryons is left over. For ADM, an initial asymmetry between dark matter particles χ and antiparticles $\bar{\chi}$ (assuming $\chi \neq \bar{\chi}$) leads to a relic density of χ only, while the symmetric χ - $\bar{\chi}$ density annihilates away. Examples of ADM candidates include technibaryons [42, 62], scalar neutrinos [63], or exotic fermions [44], as well as a wide variety of other possibilities (see Refs. [64, 65] for reviews). The baryon and dark matter asymmetries may be related, e.g., through higher-dimensional operators [46], offering a unified origin for the generation of both dark and visible matter. The cosmic ratio of dark matter-to-baryons is given by $\Omega_{\text{DM}}/\Omega_b \sim m_\chi/m_p$, where m_p is the proton mass. ADM can explain the apparent coincidence between the similar energy densities of dark and visible matter in the Universe ($\Omega_{\text{DM}}/\Omega_b \sim 5$) if the dark matter mass is in the range $m_\chi \sim 1 - 20$ GeV. Another requirement is that the $\chi\bar{\chi}$ annihilation cross section must be larger than for a typical WIMP to annihilate away the symmetric density. Indirect detection signals through annihilation today are typically absent, since only χ is present in dark matter halos today. However, accumulation of ADM in old stars can lead to observable effects [66–69]. ADM can also produce other exotic signatures; e.g., ADM in the local halo may annihilate with visible baryons, producing signals in nucleon decay searches [70].

6. Non-thermal WIMPs

It is possible that the dark matter might not be a thermal relic of the early universe, but was instead produced through a non-thermal mechanism. For example, decays of relatively long-lived stable species could produce WIMPs well after they would have ordinarily frozen out of equilibrium. Although neutralinos produced via the decay of moduli [71] or Q-balls [72] represent well-studied examples of non-thermal WIMP production, many other scenarios are also possible (e.g., [73, 74]).

7. Hidden Sector Dark Matter

In hidden sector dark matter scenarios, the dark matter does not interact through the forces of the standard model, but is instead charged under new “dark” gauge symmetries. In the early Universe, dark gauge bosons provide a thermal bath and a hidden sector experiences its own thermal history, distinct from that of the visible sector [75]. Hidden sector dark matter can have a rich structure with interesting features that usual WIMPs do not carry. In many hidden sector dark matter models, dark gauge forces mediate dark matter strong self-interactions that are relevant for astrophysics [40, 76–79]. Dark radiation can delay dark matter kinetic decoupling and suppress the matter power spectrum in small scales [40, 80]. In contrast to the WIMP paradigm, hidden sector dark matter candidates are not limited to fundamental particles, but could instead consist of composite states, such as hidden atoms [41, 80] or mirror baryons [81, 82]. The dark matter could also be made up of multiple components, with a small fraction being dissipative and forming a dark disk [83]. These novel features can leave observable signatures on structure formation by modifying the internal structure of halos, as well as the number of halos of a given mass (for the case with dark radiation). In addition, hidden sector dark matter could also couple to the standard model in the presence of a connector sector, such as the Higgs portal [84], kinetic mixing [85], or mass mixing of gauge bosons [86, 87]. In such cases, hidden sector dark matter provide signals in direct and indirect detection experiments [88–90].

III. THE FOUR PILLARS OF DARK MATTER DETECTION

A. Direct Detection

1. Scattering of WIMPs on nuclei

Dark matter permeates the whole Universe, and its local density on Earth is known to be $7 \times 10^{-25} \text{ g/cm}^3$ (0.4 GeV/cm^3) to within a factor of 2. This creates the opportunity to detect dark matter particles *directly* as they pass through and scatter off normal matter [91]. Such events are extremely rare, and so the direct detection approach requires sensitive detectors with exquisite background rejection. The expected signals and prospects for discovery depend on the nature of the dark matter particles and their interactions. For a list of current and planned experiments, see Ref. [92].

If the dark matter consists of WIMPs, direct searches are extremely promising. It has long been appreciated that if the WIMPs’ coupling to quarks is chosen such that the resulting thermal relic abundance is consistent with the observed dark matter density, the same couplings would lead to potentially detectable scattering cross sections with nuclei [91]. As the sensitivity of direct detection experiments has improved, many otherwise viable dark matter candidates have been ruled out. Of particular interest are WIMPs in the form of a scalar or a Dirac fermion which annihilates primarily through a coupling to the Z (such as a sneutrino, KK neutrino, or stable fourth generation neutrino). Such dark matter candidates are currently ruled out by direct detection constraints by multiple orders of magnitude. Excitingly, WIMPs which annihilate largely through Higgs exchange in the early universe (including neutralinos in many supersymmetric models) predict direct detection rates which are near the sensitivity of current experiments.

Experimental techniques employed in direct searches include detectors that record combinations of ionization, scintillation light, and phonons (heat). The most sensitive detectors employ multiple techniques, enabling for discrimination between dark matter scattering events and backgrounds. Depending on the target material, direct detection experiments are sensitive to a combination of

spin-dependent and spin-independent interactions between dark matter and nuclei. The sensitivity of the current generation of detectors for spin-independent scattering with protons or neutrons is approaching $\sigma_{\text{SI}}^{p,n} \sim 10^{-45} \text{ cm}^2$ for WIMP masses of $\sim 100 \text{ GeV}$. The sensitivity of the leading direct detection experiments is expected to further improve by multiple orders of magnitude over the coming decade. Although direct detection is more difficult for dark matter particles with $\sim 1\text{--}10 \text{ GeV}$, there has recently been significant progress in developing experiments with low threshold energies. More details on the current and planned experiments can be found in the Cosmic Frontier subgroup 1 (CF1) report.

2. Direct Axion Searches

Axions also have strong prospects for direct detection. Cosmological and astrophysical constraints restrict the allowed axion mass range to be between approximately $1 \mu\text{eV}$ and 1 meV . In a static magnetic field, there is a small probability for cosmologically produced axions to be converted by virtual photons to real microwave photons by the Primakoff effect [57]. This would produce a monochromatic signal with a line width of $dE/E \sim 10^{-6}$, which could be detected in a high- Q microwave cavity tunable over GHz frequencies. In the near future, such searches will be sensitive to models with axion mass $\sim \mu\text{eV}$, which is the favored region if axions are to constitute a significant component of the dark matter. More details can be found in the reports of the Cosmic Frontier subgroups 1 and 3.

B. Indirect Detection

Even if WIMPs are stable in isolation, they may undergo pair annihilation, producing energetic photons, neutrinos, and cosmic rays. Alternatively, if the dark matter is unstable, their decays could produce energetic standard model particles. A wide variety of efforts to detect such annihilation or decay products are currently underway (current and planned indirect search experiments are listed in [93]). We provide a short summary of the methods below to set the stage for the discussion on complementarity. More details can be found in the Cosmic Frontier subgroup 2 (CF2) report.

The most stringent and broadly applicable constraints on the dark matter annihilation cross section (or lifetime) have been derived from gamma-rays observations from the Fermi Gamma-Ray Space Telescope (FGST) and ground based gamma-ray telescopes. To date, Fermi data has been used to search for dark matter annihilation products from dwarf spheroidal galaxies [94, 95] and the Galactic Center [96] (as well less restrictive constraints from observations of galaxy clusters, the Galactic Halo, galactic subhalos, and the isotropic gamma-ray background). These constraints are beginning to probe annihilation cross sections at or around the value predicted for a simple thermal relic ($\sigma_{\text{th}} v \sim 3 \times 10^{-26} \text{ cm}^3/\text{s}$), at least for dark matter particles with masses below a few tens of GeV and which annihilate to final states which result in significant fluxes of gamma-rays. And while the particle (or particles) that make up the dark matter certainly could possess an annihilation cross section that is well below this value, the range of cross sections that is presently being probed by Fermi represents a very well motivated and theoretically significant benchmark. Although the strongest current constraints for significantly heavier dark matter candidates, (provided by ground based telescopes [97–101]) are not yet at the sensitivity to probe this benchmark value, the future CTA array is expected to be able to reach this level of sensitivity for WIMPs with masses between $\sim 200 \text{ GeV}$ and several TeV.

Searches for dark matter annihilation or decay products in the cosmic ray spectrum has received a great deal of attention in recent years, motivated in large part by the unexpectedly high flux of cosmic ray positrons observed by the PAMELA experiment [102] (and now confirmed with high

precision by AMS [103]). And although dark matter models have been proposed that could account for this signal, the observed positrons may also originate from nearby pulsars or other astrophysical objects [104]. Even if dark matter is not responsible for the large high-energy cosmic ray positron flux, however, the lack of sharp features in this spectrum can be used to place fairly stringent constraints on the dark matter annihilation cross section to electron-positron or muon-antimuon pairs [105]. In this respect, cosmic ray positron measurements are complementary to gamma-ray searches for dark matter, which are most sensitive to other annihilation channels. Measurements of the cosmic ray antiproton spectrum [106] are also sensitive to the annihilating dark matter at a level that is competitive with existing gamma-ray constraints. When cosmic ray and gamma-ray measurements are combined with multi-wavelength observations, such as those from radio and X-ray telescopes, it can provide a powerful means of disentangling would-be dark matter signals from astrophysical backgrounds.

Although dark matter annihilations in the galactic halo produce too few neutrinos to be detected in most models, annihilations which occur in the center of the Sun could potentially generate an observable flux of high energy neutrinos. Dark matter particles scatter with nuclei and become captured in the Sun at a rate determined by the WIMP's elastic scattering cross section. In many models, equilibrium can be reached between the capture and annihilation rates; in this case, the resulting neutrino flux does not depend on the annihilation cross section of the dark matter. For this reason, neutrino telescopes probe very different characteristics of the dark matter than other indirect search strategies. In the case in which the dark matter scatters with nuclei largely through spin-dependent couplings, the current constraints from the IceCube experiment are competitive with direct detection searches [107]. The Sun is also a potential source of dark matter axions produced in the Primakoff conversion of plasma photons. Such solar axions could be detected when they re-convert in the magnetic field of a detector on the Earth [108].

Dark matter annihilations taking place during the epoch of reionization could potentially produce a sufficient number of energetic particles to observably impact the anisotropies of the cosmic microwave background [109–111]. Measurements from WMAP and Planck provide constraints that are only modestly weaker than those derived from gamma-ray observations, and without many of the astrophysical uncertainties associated with such approaches [112].

The various indirect detection strategies described in this section are in many ways highly complementarity, potentially providing different information, being sensitive to different dark matter candidates, and suffering from different astrophysical uncertainties. For example, while interpretations of cosmic ray positron measurements rely on models of the Milky Way's magnetic field, radiation field, and gas distributions, gamma-ray observations are not sensitive to such factors (gamma-rays travel without deflection, and with negligible energy losses over Galactic scales). Gamma-ray constraints on dark matter annihilation do, however, depend on the dark matter distributions in the inner regions of halos, and on our ability to understand or model the relevant astrophysical backgrounds. Similarly, while positron measurements are very sensitive to dark matter particles which annihilate directly to electron-positron pairs but are far less sensitive to scenarios in which the WIMPs annihilate to quarks, the inverse is true for gamma-ray searches.

C. Particle Colliders

Dark matter may also be produced in high-energy particle collisions. For example, if dark matter has substantial couplings to nuclear matter, it can be created in proton-proton collisions at the Large Hadron Collider (LHC). Once produced, dark matter particles will likely pass through detectors without a trace, but their existence may be inferred from an imbalance in the visible momentum, just as in the case of neutrinos. Searches for dark matter at the LHC are therefore

typified by missing momentum, and can be categorized by the nature of the visible particles that accompany the dark matter production. Because backgrounds are typically smaller for larger values of missing momentum, collider searches tend to be most effective for low-mass dark matter particles, which are more easily produced with high momentum.

There are two primary mechanisms by which the LHC could hope to produce dark matter together with hadronic jets (see, e.g., Chapters 13 and 14 of Ref. [17]). In the first, two strongly interacting parent particles of the dark matter theory are produced, and each one subsequently decays into the dark matter and standard model particles, resulting in missing momentum plus two or more jets of hadrons. Since the production relies on the strong force, the rate of production is specified by the color charge, mass, and spin of the parent particles and is typically rather insensitive to the mass of the dark matter itself. Current null results from LHC searches for the supersymmetric partners of quarks exclude such particles with masses less than ~ 1.5 TeV.

A second mechanism produces the dark matter directly together with additional radiation from the initial quarks or gluons participating in the reaction, resulting in missing momentum recoiling against a single “mono-jet.” Since this process does not rely as explicitly on the existence of additional colored particles that decay into dark matter, it is somewhat less sensitive to the details of the specific theory and places bounds directly in the parameter space of the dark matter mass and interaction strength. However, one does need to posit a specific form of the interaction between the dark matter and quarks or gluons. For electroweak-size couplings and specific choices of the interaction structure, these searches exclude dark matter masses below about 500 GeV.

High energy lepton colliders may create dark matter through analogous processes, such as production of dark matter along with a photon radiated from the initial leptons. For electroweak-size couplings of dark matter to electrons, LEP excluded dark matter masses below about 90 GeV. A future high-energy lepton collider could conceivably discover dark matter particles with masses up to roughly half the collision energy, *e.g.*, 500 GeV for a 1 TeV ILC. For a list of current and proposed future colliders, see [113].

D. Astrophysical Probes

Many dark matter candidates, such as neutralinos, are cold and effectively collisionless (i.e., gravitational interactions dictate the resulting large scale structure). The adjective “cold” implies that the temperature of dark matter at formation is such that it allows for structure to form with masses orders of magnitude below that of the smallest galaxies observed. Predictions for cold, collisionless dark matter (CDM) agree very well with cosmological data [15], but CDM may be an approximation that breaks down on small (galactic and sub-galactic) scales. Thus, observations on galactic scales provide an opportunity to detect or constrain the possibility of dark matter that is warm or strongly self-interacting.

In recent years, observations have suggested that the central densities of some dark matter halos may be lower than expected. In particular, evidence for low central densities has been seen in a variety of self-gravitating systems, including satellite galaxies of the Milky Way, spiral galaxies, and clusters of galaxies. (See section V D for a short discussion.) Although such low density cores naively appear to be in conflict with the simplest predictions for cold, collisionless dark matter, it has been argued that baryonic feedback (such as outflows from supernovae, or the environment of galaxies) may be able to reconcile such disparities (see *e.g.*, [114]). Alternatively, these observations may be indicating that the dark matter is not entirely cold and collisionless, but may instead be either warm or strongly self-interacting.

A key prediction of collisional and collisionless cold dark matter is the presence of thousands or more dark subhalos (self-bound clumps of dark matter) within the halo of galaxies like the Milky

Way [115–117]. In order to confirm a candidate like the WIMP as being all of dark matter, it is essential to verify this prediction. A clear lack of the expected number of dark subhalos would show that the dark matter is “warm.” Compared to cold dark matter, models of warm dark matter predict less power in small-scale density fluctuations, dramatically reducing the predicted number of low-mass dark matter halos. Hidden sector models in which the dark matter interacts with other light particles can also lead to similar effects. The mass-scale below which halo formation is suppressed is directly related to one or more parameters of the particle physics model — for example, mass and couplings of sterile neutrino dark matter candidates [118]. In addition, although the central densities of dark matter halos are reduced in warm dark matter cosmology, large constant density cores have not been shown to form.

The key prediction of thousands of cold dark matter subhalos can be tested in the future using strong gravitational lensing systems, precise observations of the clustering in the universe and searches for new satellite galaxies and stellar streams. Proposed future observatories such as LSST [119] and WFIRST [120] will be able to make decisive advances towards testing this prediction, with the following expected goals.

- A deep wide-field survey should lead to the discovery of new ultra-faint satellites of the Milky Way.
- A high latitude survey will allow proper motions of halo stars at distances of 100 kpc to be measured, which will allow the mass of the Milky Way to be estimated better. This is important because issues with small-scale structure based on arguments about Milky Way’s satellite population depend sensitively on the mass of the Milky Way.
- Measuring proper motions of stars in streams associated with globular clusters like Pal 5 created by the tides of the Milky Way will allow the gaps in these streams to be characterized. Dark subhalos passing through streams will create gaps and the nature of these gaps could reveal the presence of subhalos down to a million solar masses, for which there are no visible counterparts [121].
- Huge increase in the number of strong lenses observed will allow the inner structure (radial profile and shape) of dark matter halos in the lensing galaxies, groups of galaxies and clusters of galaxies to be studied with unprecedented accuracy.
- The wide field-of-view will allow rare mergers of extremely massive clusters to be photographed and the depth and angular resolution will allow for a detailed mapping of dark matter matter in multiple merging clusters, perhaps rivaling the Bullet Cluster.

For some of the above goals LSST is better suited, while for others it is WFIRST. We refer the reader to the science cases for LSST and WFIRST [119, 120] for more details and references.

Strong lensing is the most direct way to “image” dark subhalos. A true measurement of the subhalo abundance in a galaxy using strong lensing will require a separate effort from future wide and deep galaxy surveys. Three promising methods, each with its own systematics but capable of measuring dark clumps with masses around $10^8 M_\odot$ or lower, have been discussed recently. Presence of a small clump near an arc created by strong lensing of a background galaxy can distort the surface brightness distribution of the arc from being smooth (locally). This localized deviation from smoothness can be used to place constraints on the mass of the clump in lenses at cosmological distances [122]. The time delays between multiple images created by gravitational lensing can be measured by monitoring sources like active galactic nuclei (AGN) that vary over time. These time delays are sensitive to substructure [123] and a mission OMEGA [124] has been proposed to measure the substructure fraction in galaxies using time delays. A third method advocates

using radio telescopes (like ALMA) to detect gravitational lensing of dusty, star forming galaxies bright in sub-mm wavelengths. With spectroscopy, it is expected that gravitational lensing of these bright, dusty, star forming galaxies is akin to having multiple sources (at the same redshift) being lensed by a foreground galaxy, increasing the signal to noise dramatically [125].

The lack of substructure, if any, should also be visible in the power spectrum measurements. In the past, this has been accomplished through the measurements of correlations in the Ly- α forest formed by absorption in neutral hydrogen clouds along the line of sight to quasars. It has been argued that the constraints from Ly- α preclude warm dark matter from solving any of the small-scale structure problems [126, 127]. The main uncertainties in this method have to do with the unknown properties of the intergalactic medium [128]. This is an issue that is systematics limited since the current sample of quasars is already huge [129] and will grow by an order of magnitude or more. In order to make progress, this method will require significant advances in the analysis methods and theory work including numerical simulations of the intergalactic medium.

In comparison to warm dark matter, the primary effect of self-interactions of dark matter is to reduce the central density of dark matter halos and create constant density (spherical) cores. Such effects would be expected to be observable if the cross section to particle mass ratio is of order $1 \text{ cm}^2/\text{g}$ ($0.2\text{--}2 \times 10^{-24} \text{ cm}^2/\text{GeV}$) [117, 130, 131]. Cross sections of this magnitude can be produced in hidden sector dark matter models through the exchange of a light gauge boson and this interaction can also endow the dark matter particle with the desired relic density [77]. In these cases, the Bullet Cluster constraints [132] are typically weak because of the intrinsic velocity dependence of the cross section in these (and most other) models. This and other aspects of complementarity between direct searches for self-interacting dark matter and astrophysics are discussed further in section V D.

In addition to structure formation, non-gravitational interactions of dark matter could impact a variety of other astrophysical phenomena. For example, coupling of axions and light sterile neutrinos (or generally any light hidden-sector particles) to standard model particles may affect the cooling of compact objects (stars, neutron stars, white dwarfs, supernovae) [133] or, decays or annihilations of dark matter particles could affect the process of reionization of neutral atoms, which took place in the first billion years after the Big Bang [134].

While dark matter physics may have imprinted tell-tale astrophysical signatures, it will be hard to unambiguously identify such signatures as non-gravitational interactions of dark matter. The complementarity with direct, indirect or collider searches is an essential part of this endeavor.

IV. QUALITATIVE COMPLEMENTARITY

The various techniques and detection strategies described in the previous section are each able to provide different and complementary information about the nature dark matter. These experimental approaches are each able to measure or constrain different aspects of the dark matter's interactions and other characteristics, and are in many cases sensitive to different classes of dark matter candidates. Furthermore, these different strategies are each limited by different astrophysical, instrumental, and other uncertainties. And while it may be unlikely than any one experimental endeavor will conclusively identify the particle nature of dark matter, a diverse array of experiments and observations could potentially bring together a collection of information over the coming decade that might bring resolution to the long-standing question of dark matter.

At a qualitative level, the complementarity between these categories of dark matter search strategies is illustrated by the following observations that follow from the basic features of each approach:

- *Direct Detection* is perhaps the most straightforward detection method, with excellent

prospects for improved sensitivity in the coming decade and for discovering WIMPs. The approach requires careful control of low-energy backgrounds, and is relatively insensitive to dark matter that couples to leptons only, or to WIMP-like dark matter with mass ~ 1 GeV or below. Ultimately, direct detection experiments could constrain the dark matter particle’s mass, and its elastic scattering cross sections with protons and neutrons (modulo uncertainties in the local dark matter density).

- *Indirect Detection* is potentially sensitive to dark matter interactions with all standard model particles, through combinations of gamma-ray, cosmic ray, neutrino, and multi-wavelength observations. These approaches are currently beginning to probe dark matter particles with annihilation cross sections similar to that predicted for a simple thermal relic, and experimental sensitivities are expected to improve significantly on several fronts within the coming decade. Discovery through indirect detection requires understanding of astrophysical backgrounds, and prospects are often subject to uncertainties in the dark matter distribution.
- *Particle Colliders*, such as the Large Hadron Collider, provide the opportunity to study dark matter in a highly controlled laboratory environment, and are potentially sensitive to a wide variety of dark matter models. Hadron (lepton) colliders are relatively insensitive to dark matter that interacts only with leptons (hadrons). Unlike direct and indirect astrophysical searches for dark matter, colliders will not be able to determine whether any newly discovered weakly interacting particle is stable and cosmologically relevant, or merely long-lived on the timescales relevant to its detectors (~ 100 ns).
- *Astrophysical Probes* can be sensitive to the “warmth” of dark matter and to properties such as its self-interaction strength. By measuring the impact of the dark matter properties on the structure formation of the Universe, astrophysical probes may be able to identify departures from the cold, collisionless dark matter paradigm.

V. QUANTITATIVE COMPLEMENTARITY

A. Effective Operator Description

Many of the qualitative features outlined above can be illustrated in a simple and fairly model-independent setting by considering dark matter that interacts with standard model particles through four-particle contact interactions, which represent the exchange of very heavy particles. While not entirely general, these contact interactions are expected to work well to describe theories in which the exchanged particle mass is considerably larger than the momentum transfer of the physical process of interest.

In this toy exercise, we consider a spin-1/2 dark matter particle, χ , with the following generation-independent interactions to quarks q , gluons g , and leptons ℓ (including neutrinos), respectively:

$$\frac{1}{M_q^2} \bar{\chi} \gamma^\mu \gamma_5 \chi \sum_q \bar{q} \gamma_\mu \gamma_5 q + \frac{\alpha_S}{M_g^3} \bar{\chi} \chi G^{a\mu\nu} G_{\mu\nu}^a + \frac{1}{M_\ell^2} \bar{\chi} \gamma^\mu \chi \sum_\ell \bar{\ell} \gamma_\mu \ell. \quad (1)$$

Although we could have chosen many other interactions (e.g., operators with different Lorentz structures, or involving other SM particles), these three are reasonably representative examples which capture many of the phenomenological features most relevant for dark matter searches [135]. For example, the interactions with quarks described above lead to spin-dependent elastic scattering with nuclei, while the interaction with gluons mediates a spin-independent interaction. The coefficients M_q , M_g , and M_ℓ each characterize the strength of the interaction with the respective standard model particle. The values of the three interaction strengths, together with the mass of the dark matter particle, m_χ , completely define this theory (at sufficiently low energies) and

allow one to predict the rates of both spin-dependent and spin-independent direct scattering, the annihilation cross sections into quarks, gluons, and leptons, and the production rate of dark matter at colliders [135–142].

Each class of dark matter search outlined in Sec. III is sensitive to some range of the interaction strengths for a given dark matter mass. Therefore, they are all implicitly capable of putting a bound on that interaction’s contribution to the annihilation cross section into a particular channel. Since the annihilation cross section at the temperature of freeze-out predicts the dark matter relic density, the reach of any experiment is thus equivalent to a fraction of the observed dark matter density Ω_{DM} . This connection can be seen in the plots in Fig. 2, which show the annihilation cross sections $\sigma_i(M_i)$, ($i = g, q, l$) for each individual channel, normalized to the value σ_{th} required¹ for a single thermal WIMP

$$\frac{\sigma_i(M_i)}{\sigma_{\text{th}}} = \frac{f_i}{\Omega_\chi/\Omega_{\text{DM}}}, \quad (2)$$

where

$$f_i \equiv \frac{\sigma_i(M_i)}{\sigma_{\text{total}}} \leq 1 \quad (3)$$

is the fractional contribution of the particular channel i to the total annihilation cross-section $\sigma_{\text{total}} \equiv \sigma(\chi\chi \rightarrow \text{anything})$.

Assuming $f_i = 1$ (i.e., that an individual channel i saturates the total annihilation cross-section σ_{total}), σ_{th} provides a natural target for dark matter searches: if the discovery potential for an experiment reaches cross sections $\sigma_i \sim \sigma_{\text{th}}$ (the horizontal dot-dashed lines in Fig. 2), that experiment will be able to discover a thermal relic which could potentially (with the assumption of $f_i = 1$) account for all dark matter in the universe. On the other hand, if an experiment were to observe an interaction consistent with an annihilation cross section σ_i below σ_{th} (yellow-shaded regions in Fig. 2), it would have discovered dark matter, but through an interaction that cannot alone account for the observed relic abundance. In that situation, $\Omega_\chi \sim \Omega_{\text{DM}}$ can be achieved only with $f_i < 1$ and therefore, additional interactions contributing to other annihilation channels in addition to i must have been present in the early universe. Finally, if an experiment were to observe a cross section σ_i above σ_{th} (green-shaded regions in Fig. 2), this discovery could point to a multicomponent dark matter scenario, in which the χ species is only one among several dark matter particles ($\Omega_\chi < \Omega_{\text{DM}}$). Alternatively, it can also be suggestive of dark matter with a non-thermal origin (in which case eq. (2) does not apply), or of dark matter with interactions that are not well-described by the effective operator approach of eq. (1). Further discussion can be found in Refs. [143–151].

In Fig. 2, we assemble the current bounds (solid lines) and discovery potential (dashed lines) for several near-term dark matter searches that are sensitive to interactions with gluons, quarks, or leptons. It is clear that the searches are complementary to each other in terms of being sensitive to interactions with different standard model particles. These results also illustrate that within a given interaction type, the reach of different search strategies depends sensitively on the dark matter mass. For example, direct searches for dark matter are very powerful for masses around 50 GeV (even in the lepton scenario, due to loop-mediated γ and Z exchanges [158]), but have difficulty at very low masses, where the dark matter particles carry too little momentum to noticeably affect heavy nuclei. This region of low mass is precisely where collider production of dark matter

¹ For non-thermal WIMPs or asymmetric dark matter, the annihilation cross-section does not have a naturally preferred value, but the plots in Fig. 2 are still meaningful.

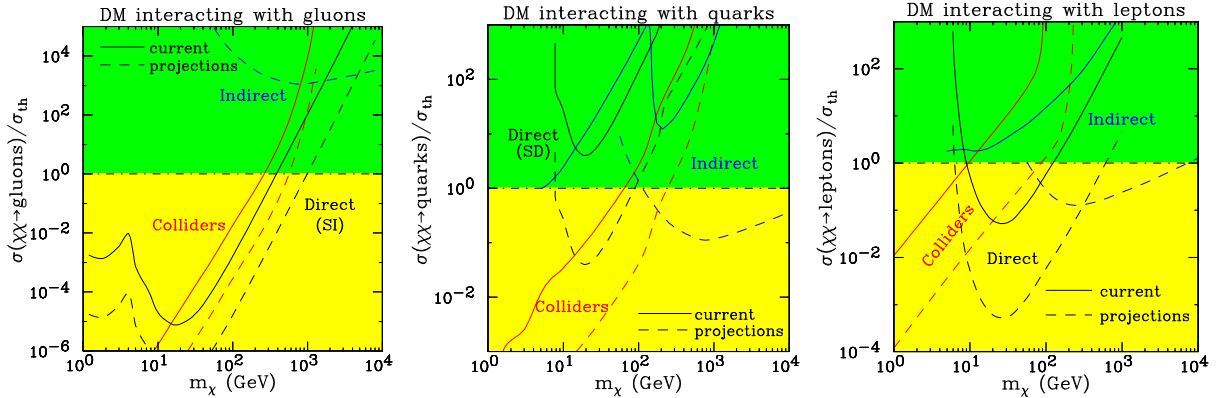


FIG. 2: Dark matter discovery prospects in the $(m_\chi, \sigma_i/\sigma_{\text{th}})$ plane for current and future direct detection [152], indirect detection [95, 153], and particle colliders [154–156] for dark matter coupling to gluons [137], quarks [137, 157], and leptons [158, 159], as indicated.

is expected to be most promising, since high energy collisions readily produce light dark matter particles with large momenta. Fig. 2 confirms that the difficult low-mass region is effectively covered by searches at the LHC (in the case of gluon or quark couplings) or at LEP and ILC (in the case of lepton couplings). The sensitivity of both direct searches and colliders is increasingly diminished at high masses, and this is where indirect detection probes play an important complementary role — in the case of couplings to quarks and leptons, CTA arrays are able to cover the relevant parameter region in the mass range around 1 TeV.

B. Supersymmetry

The effective theory description of the dark matter interactions with standard model particles discussed above is an attempt to capture the salient features of the dark matter phenomenology without reference to any specific theoretical model. However, the complementarity between the different dark matter probes illustrated in Fig. 2 is also found when one considers specific theoretical models with WIMP dark matter candidates. Among the many other alternatives, low energy supersymmetry [160] and models with universal extra dimensions (UED) have been a popular and widely studied extensions of the standard model. In the following, we will discuss the interplay between different dark matter detection strategies within the context of supersymmetric and UED models.

1. The phenomenological MSSM (pMSSM)

Even within the general context of low-energy supersymmetry, there are many different scenarios that can be considered. Philosophically, these scenarios tend to fall within either top-down or bottom-up approaches. In top-down models, the low-energy sparticle spectrum is derived from a high-energy theory, which relies on various theoretical assumptions, but typically requires relatively few input parameters. Alternatively, one can phenomenologically describe the properties of the low-energy sparticle spectrum with fewer theoretical assumptions, but with a greater number of input parameters. We begin this discussion of complementarity within the context of supersymmetric dark matter by considering a phenomenological approach to the minimal supersymmetric standard model (MSSM), based on the results presented in [161], before turning our attention to more

$m_{\tilde{L}(e)_{1,2,3}}$	100GeV – 4TeV
$m_{\tilde{Q}(q)_{1,2}}$	400GeV – 4TeV
$m_{\tilde{Q}(q)_3}$	200GeV – 4TeV
$ M_1 $	50GeV – 4TeV
$ M_2 $	100GeV – 4TeV
$ \mu $	100GeV – 4TeV
M_3	400GeV – 4TeV
$ A_{t,b,\tau} $	0GeV – 4TeV
M_A	100GeV – 4TeV
$\tan\beta$	1 - 60
$m_{3/2}$	1 eV–1TeV (\tilde{G} LSP)

TABLE I: Scan ranges for the 19 (20) parameters of the pMSSM with a neutralino (gravitino) LSP. The gravitino mass is scanned with a log prior. All other parameters are scanned with flat priors, though this choice is expected to have little qualitative impact on the results [162–164].

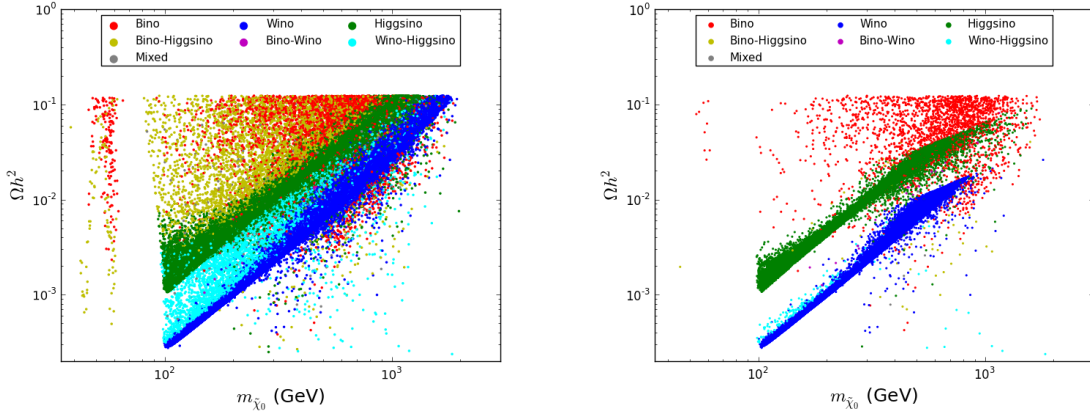


FIG. 3: Left: Thermal relic density as a function of the LSP mass in the pMSSM model set, as generated, color-coded by the electroweak properties of the LSP as discussed in the text. Right: Thermal relic density as a function of the LSP mass for all pMSSM models, surviving after all searches, color-coded by the electroweak properties of the LSP.

concrete theoretical scenarios later on.

In the pMSSM approach, one scans over all phenomenologically relevant input parameters and considers all models which pass the existing experimental constraints and have a dark matter candidate which can account for at least a portion of the observed dark matter density [165–167]. The pMSSM parameters and the ranges of values employed in the scans are listed in Table I, where the lower and upper limits were chosen to be essentially consistent with Tevatron and LEP data and to have kinematically accessible sparticles at the LHC, respectively. To study the pMSSM, many millions of model points were generated in this space (using SOFTSUSY [168] and checking for consistency with SuSpect [169], while the decay patterns of the SUSY partners and the extended Higgs sector are calculated using a modified version of SUSY-HIT [170]). These individual models are then subjected to a large set of collider, flavor, precision measurement, dark matter and theoretical constraints [165].

Roughly 225k models with a neutralino LSP survive this initial selection and can then be used for further physics studies. The left panel in Figure 3 shows the thermal relic densities of the

LSPs in the pMSSM model sample as a function of their mass, with suitable color-coding reflecting their electroweak eigenstate content as indicated in the figure. Figure 3 illustrates essentially every possible mechanism to obtain (or lie below) the required relic density Ω_{DM} : (i) The set of points at low masses forming “columns” corresponds to bino and bino-Higgsino admixtures surviving due to their proximity to the Z and h -funnels, where the annihilation cross-section is resonantly enhanced. (ii) The gold-colored points saturating the relic density in the upper left represent models with bino-Higgsino LSPs of the so-called “well-tempered” variety. (iii) the red pure² bino models in the middle top of the Figure are bino co-annihilators (mostly with sleptons) or are models near the A -funnel region. (iv) The green (blue) bands are pure Higgsino (wino) models that saturate the relic density bound near $\sim 1(1.7)$ TeV but dominantly appear at far lower relic densities. Wino-Higgsino hybrids are seen to lie between these two cases as expected.

Within each model, the dark matter interactions are completely specified and one can readily compute all relevant dark matter signals. Fig. 4 shows the survival and exclusion rates resulting from the various searches and their combinations in the plane of the LSP mass versus the spin-independent direct detection cross section, scaled by a factor $R = \Omega_\chi/\Omega_{\text{DM}}$ to account for the fact that most of the pMSSM models lead to a thermal relic density somewhat below the measured value Ω_{DM} . The models are categorized depending on the observability of a dark matter signal in direct detection experiments (green points), indirect detection experiments (blue points) or both (red points). The left panel in Fig. 4 contrasts direct detection (DD) and indirect detection (ID) searches. Note that the DD- and ID-excluded regions are relatively well separated in terms of mass and cross section although there is also some overlap between the sets of models excluded by the different experiments. This nicely illustrates the complementarity between DD and ID probes: at low and moderate masses, the DD experiments cover a large fraction of models (green points) which would otherwise evade indirect detection. At the same time, at high masses, a sizable fraction of models (the blue points) can only be seen in indirect detection (via ground-based gamma ray telescopes). The red points represent models for which one would have an independent confirmation of a dark matter signal by two different types of probes. Among the models which escape detection in DD and ID dark matter experiments, some (the magenta points in Fig. 4) are already ruled out by current LHC data while others (the remaining grey points) will potentially be probed after the LHC upgrade (the analysis of the projected sensitivity of the upgraded LHC is still ongoing). Figure 4 demonstrates that the three different dark matter probes nicely combine to discover most (albeit not all) supersymmetry models in this scan.

The models which survive all searches are categorized in the right panel of Fig. 3, which should be compared with the original model set as generated in the left panel of Fig. 3. One can see that (i) the models in the light h and Z -funnel regions have essentially evaporated (and further measurements of the invisible width of Higgs as well as the standard SUSY searches will likely further restrict these), (ii) the well-tempered neutralinos are now seen to be completely gone; (iii) the possibility of almost pure Higgsino or wino LSPs even approximately saturating the relic density has vanished thanks to CTA, (iv) the mixed wino-Higgsino models, due to a combination of measurements, have also completely disappeared. (v) The only models remaining which *do* saturate the WMAP/Planck relic density are those with bino co-annihilation.

2. Specific MSSM scenarios

One of the driving motivations for supersymmetry (SUSY) theories is the hierarchy problem of the Standard Model (SM). The presence of superpartners at the weak scale cancels quadratic

² Here ‘pure’ means having an eigenstate fraction $\geq 90\%$.

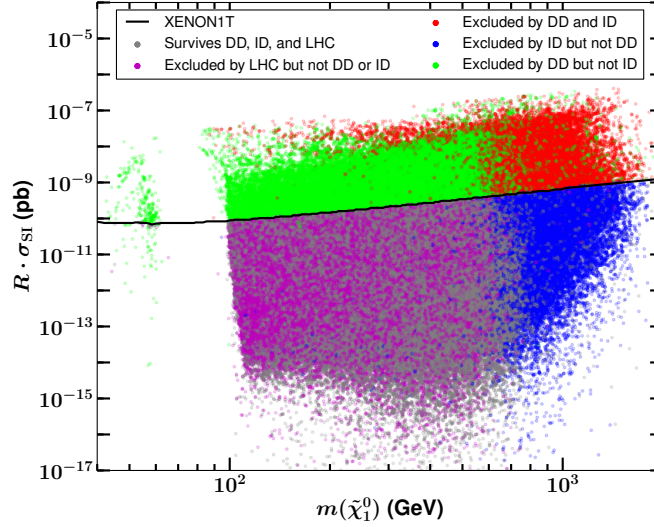


FIG. 4: Results from a model-independent scan [161, 165] of the parameter space in the minimal supersymmetric model (MSSM), presented in the $(m_{\chi}, R \cdot \sigma_{\text{SI}}^p)$ plane. The models are divided into categories, depending on whether dark matter can be discovered in future direct detection experiments (green points), indirect detection experiments (blue points) or both (red points). Among the remaining models, the magenta (grey) points represent models that will (will not) be discovered at the upgraded LHC.

divergences in the Higgs potential, drastically reducing the fine-tuning present in the theory. However, current LHC results generically imply squark masses of $\gtrsim 1$ TeV. In most SUSY models this implies a mild reintroduction of fine-tuning, which, while far less severe than the fine-tuning present in the SM, weakens the motivation of SUSY theories.

This issue is compounded by the discovery of the Higgs boson at the LHC with a mass of $m_h \approx 125.6$ GeV [171, 172]. In the MSSM, it is well-known that radiative corrections can lift the Higgs mass above the tree-level bound of $m_Z \simeq 91$ GeV. However, achieving a Higgs mass as large as the one observed experimentally requires either stop masses of $\mathcal{O}(8 - 10)$ TeV or a large stop A -term. Large A -terms are non-generic, while stop masses of $\mathcal{O}(8 - 10)$ TeV seem to reintroduce some fine-tuning.

Relatively heavy scalars are also motivated from precision observables in the flavor and CP violation sectors. General weak-scale SUSY models suffer serious constraints from flavor violating observables, which would point to a heavy sfermion sector. Even though well-known mechanisms exist to ameliorate the dangerous flavor-changing effects, in concrete models, CP violation is generally still present, and motivates sfermion masses in the multi-TeV range to avoid electron and neutron EDM constraints [173].

Focus Point Supersymmetry. One specific framework which addresses this combination of issues is focus point (FP) supersymmetry [174, 175]. In the MSSM for $\tan \beta \gtrsim 5$, electroweak symmetry breaking requires at tree level

$$m_Z^2 \approx -2\mu^2 - 2m_{H_u}^2(m_W), \quad (4)$$

where μ is the higgsino mass parameter and $m_{H_u}^2$ is the soft up-type Higgs mass parameter. The theory is relatively natural, if $m_Z^2 \sim \mu^2 \approx |m_{H_u}^2|$, which can be achieved for certain sets of boundary conditions due to renormalization group (RG) running, even when (some of) the SUSY-breaking masses are significantly larger than m_Z . One such example is the FP scenario, in which the scalar masses are universal at the GUT scale, the A -terms are negligible (see, however [176]), and the

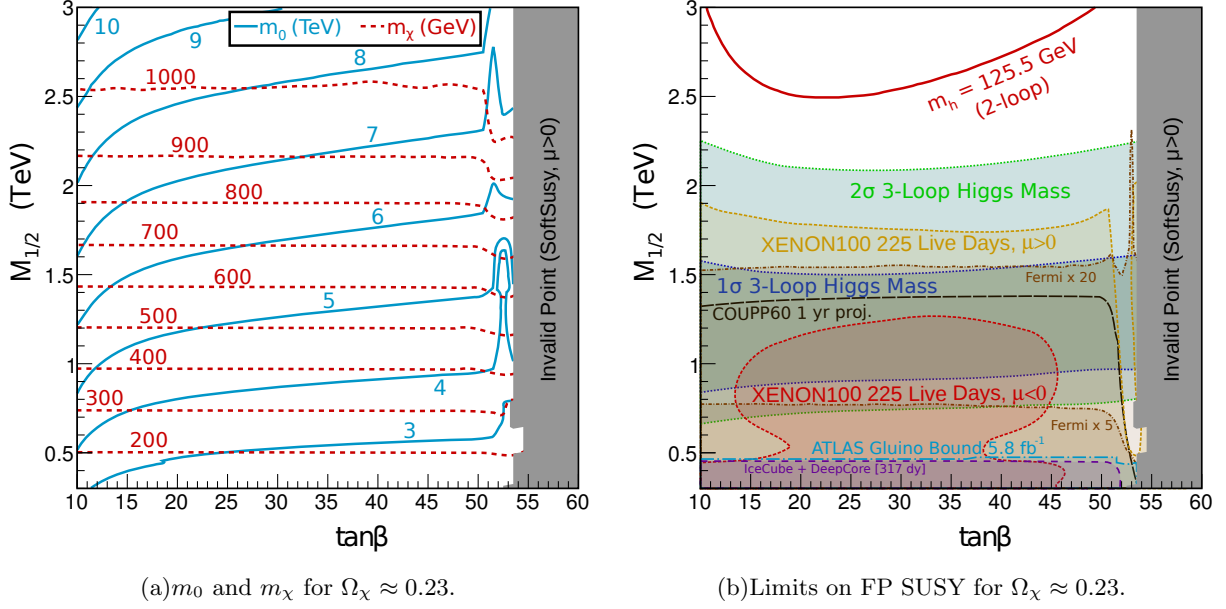


FIG. 5: *The Focus Point Region for $\Omega_\chi = \Omega_{DM}$.* Shown are the values of m_0 and m_χ satisfying the thermal relic density (left) and relevant constraints (right). The collider constraint is extrapolated from ATLAS gluino searches using 5.8 fb^{-1} of data with $\sqrt{s} = 8$ TeV [180]. Current dark matter constraints use results from XENON100 with 225 live days [181] and IceCube (w/ DeepCore) results using 317 live days [107]. Projected limits are drawn from projected COUPP60 sensitivity after a 1 year physics run [182] and multiples of the current Fermi-LAT sensitivity from a stacked dwarf spheroidal analysis [183]. The two-loop Higgs mass is determined by SOFTSUSY [168], while the three-loop result uses H3M [184, 185]. Plots are taken from Ref. [186].

gaugino masses are small. This scenario is realized in the constrained MSSM (CMSSM) with $A_0 = 0$ and $M_{1/2} \ll m_0$, producing the “focus point region” of the CMSSM where m_0 is in the multi-TeV range but μ remains near the weak scale [174, 175].

While the collider prospects for the FP region are poor due to the large superpartner masses, large portions can be probed at a variety of dark matter experiments. Given the relatively small values of μ , the FP region exhibits a mixed Bino-Higgsino LSP, which produces the right amount of dark matter. Significant Bino-Higgsino mixing also enhances both direct detection and annihilation signals, improving the ability of dark matter experiments to probe FP models [177, 178]. Spin-independent direct detection is particularly interesting for such models, with cross-sections within the reach of current and near-future direct detection experiments [179].

In exploring the FP parameter space, a particularly interesting region is the slice wherein the neutralino thermal relic density saturates the observed relic density,

$$\Omega_\chi(m_0, M_{1/2}, A_0, \tan\beta, \text{sign}(\mu)) = \Omega_{DM}. \quad (5)$$

By fixing the sign of μ and setting $A_0 = 0$ to generate the desirable FP RG behavior, for a particular choice of $\{M_{1/2}, \tan\beta\}$ there exists a unique value of m_0 for which $\Omega_\chi = \Omega_{DM}$ [187]. This allows the FP region to be studied in the $\{M_{1/2}, \tan\beta\}$ plane wherein *every point has the correct thermal relic density* [187]. By directly taking into account the cosmological constraint (5), one is able to better explore a larger portion of the relevant parameter space. Results for the FP region are shown in Figure 5, based on the relic density determination of WMAP with 7 years of data [15]. The analysis also used SOFTSUSY 3.1.7 [168] for spectrum generation, MICROMEGAS 2.4 [188] to calculate the relic density and direct detection processes, and DARKSUSY 5.0.5 [189] to calculate

indirect detection rates. Figure 5(a) shows the value of m_0 required to achieve $\Omega_\chi = \Omega_{\text{DM}}$ and the corresponding neutralino mass m_χ . Generally the required value of m_0 increases with increasing $M_{1/2}$ and decreases with increasing $\tan\beta$. However, for $\tan\beta \gtrsim 50$ the appropriate value shifts downward, as the pseudoscalar Higgs bosons becomes light enough in this region to significantly alter the relic density calculation.

Figure 5(b) shows associated constraints upon the FP region. Due to the relatively high squark mass scale, the dominant collider constraints are derived from searches for gluino pair-production [180]. The associated reach is relatively limited, constraining $M_{1/2} \lesssim 500$ GeV almost independent of $\tan\beta$. Even with current data, direct detection experiments place significantly stronger bounds, with current XENON100 [181] results constraining $M_{1/2} \gtrsim 1.8$ TeV for nearly the entire range of $\tan\beta$ shown if $\mu > 0$, with somewhat stronger bounds at large and small $\tan\beta$. For $\mu < 0$ the constraints are weaker, requiring $M_{1/2} \gtrsim 1$ TeV for a moderate range of $\tan\beta$ but weakening to $M_{1/2} \gtrsim 500$ GeV for small $\tan\beta$ and placing no constraint for $\tan\beta \gtrsim 45$. Spin-independent limits were produced using a strange quark form factor of $f_s = 0.05$ [190–192]. While current spin-dependent results do not have sensitivity to the focus point parameter space, near future results from COUPP60 [182] are expected to constrain $M_{1/2} \lesssim 1.3 - 1.4$ TeV for $\tan\beta \lesssim 50$. Indirect detection experiments are also relevant, with current IceCube [107] results constraining $M_{1/2} \gtrsim 500$ GeV for $\tan\beta \lesssim 50$, producing a bound competitive with current LHC constraints. Moreover, while gamma ray searches currently do not probe the FP region, an order of magnitude improvement on current Fermi-LAT sensitivity from dwarf spheroidals [183] will provide significant sensitivity to $M_{1/2} \sim 700$ GeV – 1.5 TeV. The generation of IceCube and Fermi-LAT bounds are detailed in Ref. [186]. Future experiments on all these fronts will have the ability to probe significantly larger regions of FP parameter space.

These sensitivities are especially important given recent computations of the Higgs mass with leading 3-loop effects included in models with multi-TeV scalars [186, 193]. Generally 2-loop determinations require stop masses of $\mathcal{O}(8-10)$ TeV, which in the FP region with $A_0 = 0$ places the appropriate Higgs mass at $M_{1/2} \gtrsim 2.5$ TeV, beyond the reach of current or near-future experiments. However, including 3-loop effects reduces the required stop mass to 3 – 4 TeV even without left-right mixing, improving the prospect of dark matter and collider experiments to probe FP models, with a favored region of $700 \text{ GeV} \lesssim M_{1/2} \lesssim 2.2 \text{ TeV}$ [186].

Radiatively-driven Natural Supersymmetry. Another way to ameliorate the fine tuning present in eq. (4) is to consider non-universal boundary conditions for the soft SUSY breaking parameters at the GUT scale. One specific such class of models resulting in a low value of the fine-tuning measure Δ_{EW} has been labeled as radiatively-driven natural supersymmetry (RNS) [194–196] (see also [197–200]). In RNS models, $\mu \sim 100 - 300$ GeV, and the lightest neutralino is largely higgsino-like, albeit with some non-negligible gaugino component. The thermally-produced relic density Ω_h^{TP} of higgsino-like WIMPs from RNS is typically found to be a factor 5 – 15 below the measured value for CDM, as shown in Fig. 6 [195, 201]. To accommodate this situation, a cosmology with mixed axion/higgsino dark matter (two dark matter particles, an axion and a higgsino-like neutralino)[202–205] has been invoked in Ref. [195, 201]. In this case, thermal production of axinos \tilde{a} in the early universe followed by $\tilde{a} \rightarrow g\tilde{g}$, $\gamma\tilde{Z}_i$ leads to additional neutralino production. In the case where axinos are sufficiently produced, their decays may lead to neutralino re-annihilation at temperatures below freeze-out; the resulting re-annihilation abundance is always larger than the standard freeze-out value. In addition, coherent-oscillation production of saxions s at high PQ scale $f_a > 10^{12}$ GeV followed by saxion decays to SUSY particles can also augment the neutralino abundance. Late saxion decay to primarily SM particles can result in entropy dilution of all relics (including axions) present at the time of decay, so long as BBN and dark radiation constraints are respected. The upshot is that, depending on the additional PQ parameters, either higgsino-like neutralinos or axions can dominate the dark matter abundance, or they may co-exist

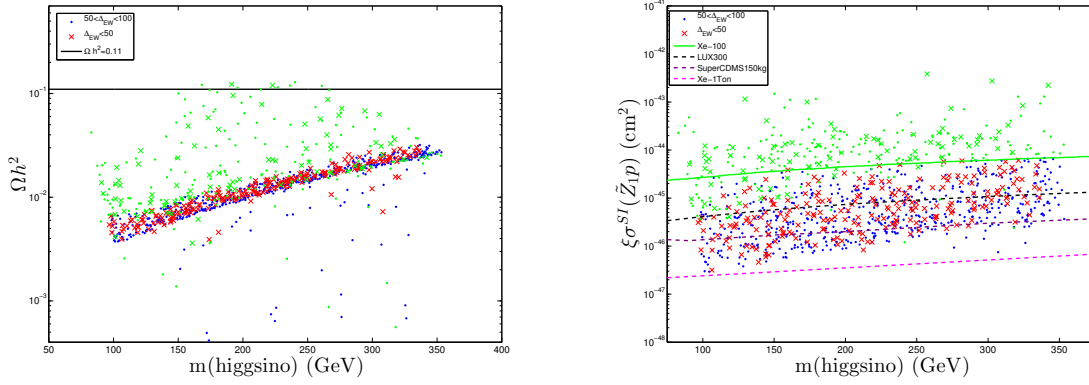


FIG. 6: Left: Plot of the standard thermal neutralino abundance $\Omega_{\tilde{Z}_1}^{TP} h^2$ versus $m(\text{higgsino})$ from a scan over NUHM2 parameter space with $\Delta_{EW} < 50$ (red crosses) and $\Delta_{EW} < 100$ (blue dots). Green points are excluded by current direct/indirect WIMP search experiments. The horizontal line shows the central value of $\Omega_{CDM} h^2$ from WMAP9. Right: Plot of rescaled higgsino-like WIMP spin-independent direct detection rate $\xi \sigma^{SI}(\tilde{Z}_1 p)$ versus $m(\text{higgsino})$ from a scan over NUHM2 parameter space with $\Delta_{EW} < 50$ (red crosses) and $\Delta_{EW} < 100$ (blue dots). Green points are excluded by current direct/indirect WIMP search experiments. Also shown are the current limits from XENON100 experiment, and projected reaches of LUX, SuperCDMS 150 kg and XENON1T.

with comparable abundances: this leads to the possibility of detecting both an axion and a WIMP (see also Section VI below).

In the case of mixed axion-WIMP dark matter, the local WIMP abundance might be well below the commonly accepted local abundance $\rho_{loc} \sim 0.3 \text{ GeV}/\text{cm}^3$. Thus, to be conservative, limits from experiments like XENON100 or CDMS should be compared to theoretical predictions which have been scaled down[206] by a factor $\xi \equiv \Omega_{\tilde{h}}^{TP} h^2 / 0.12$. In the RNS model, the gauginos cannot be too heavy so that the neutralino always has a substantial gaugino component even though it is primarily higgsino. This means that spin-independent direct detection rates $\sigma_{SI}(\tilde{Z}_1 p)$ are never too small. Predictions for spin-independent higgsino-proton scattering cross section are shown in Fig. 6 and compared against current limits and future reach projections. Even accounting for the local scaling factor ξ , it is found [201] that ton-scale noble liquid detectors such as XENON1T [207] should completely probe the model parameter space. One caveat is that if saxions give rise to huge entropy dilution after freeze-out while avoiding constraints from dark radiation and BBN, then the local abundance may be even lower than the assumed freeze-out value, and the dark matter would be highly axion dominated.

3. The Next-to-minimal MSSM (NMSSM)

Despite a great deal of attention, the MSSM is not without shortcomings, e.g. the so-called “mu-problem” is related to the presence of a term in the superpotential

$$W_{MSSM} \supset \mu H_u H_d \quad (6)$$

with a mass parameter μ which has no a-priori connection to the electroweak scale. The Next-to-Minimal Supersymmetric Standard Model (NMSSM) is a simple extension to the MSSM which tries to alleviate the mu-problem by promoting the μ parameter to a dynamical field S , replacing

FIG. 7: Relic abundance (left), scaled SI cross section (middle) and SD cross section (right) for the saturated (top) and unsaturated (bottom) DM relic abundance scenarios. Limits on σ_{SI} from Xenon100 [181], LUX [216], and Xenon 1 Ton [207], and σ_{SD} from IceCube [217]. Figures taken from Ref. [218].

(6) with

$$W_{NMSSM} \supset \lambda_S S H_u H_d + \frac{\kappa}{3} S^3, \quad (7)$$

where λ_S and κ are dimensionless parameters. When the singlet S obtains a VEV, an effective μ parameter is generated. The additional scalar superfield S in the NMSSM increases the field content, leading to another possible dark matter candidate, the singlino, \tilde{S} [208–210].

Here the status of the NMSSM with respect to current data is investigated, under the assumption of decoupled sfermions, in order to focus on the role of the singlet scalar and its superpartner, the singlino. Two cases are explored, first, where χ_1^0 can account for the dark matter relic abundance in its entirety, and second, when it is only a subdominant component. The fit requires consistency with SUSY searches [211–213] and present $h(125)$ measurements at the LHC [214, 215]. In the case of a saturated relic abundance, a 10% theoretical uncertainty on the measured value of $\Omega_{DM} h^2$ is assumed. The relic abundance for the two cases are shown in the left panels of Fig. 7.

The LHC $h(125)$ measurements indicate a SM-like Higgs boson. Therefore, if $\tan \beta \gg 1$, the lightest Higgs is typically dominated by H_u . As a consequence, the $h\chi_1^0\chi_1^0$ coupling that primarily controls σ_{SI} avoids tension with the Xenon100 exclusion if χ_1^0 is mainly bino or wino. When χ_1^0 is a wino or higgsino, the masses χ_2^0 and χ_1^\pm are comparable to χ_1^0 , leading to significant co-annihilation effects. Moreover, this scenario offers a difficult scenario at the LHC for discovering these states as the decay products will typically be soft and evade the selection cuts (recall the right panel in Fig. 3).

In the saturated relic abundance scenario, χ_1^0 can be either bino or singlino. Some key observables are illustrated in the top row of Fig. 7.

- In the bino scenario, σv_{tot} is often below $3 \times 10^{-27} \text{ cm}^3 \text{ s}^{-1}$, therefore $\chi_1^0 \chi_1^\pm$ and $\chi_1^0 \chi_2^0$ co-annihilation is required, with mass splitting of $\mathcal{O}(20 \text{ GeV})$. The SI scattering cross sections are within reach of future detectors such as Xenon 1 Ton and LUX.
- In the singlino scenario, σ_{SI} is reduced since usually dominant h exchange is suppressed by the lack of a singlet component.

In either case, the SD cross section is more than a factor of 10 below the current bound placed by COUPP [219] and IceCube [217]. A light scalar singlet with $M_s < 100 \text{ GeV}$ is possible, which may offer interesting signatures at the LHC such as $h \rightarrow ss \rightarrow b\bar{b} + b\bar{b}(\tau\tau)$.

The unsaturated case (lower row of plots in Fig. 7) is dominated by either higgsino or wino DM. In both cases, co-annihilation with the associated χ_1^\pm results in a low relic abundance, thus the direct detection sensitivities are scaled by the local density $\rho_{\chi_1^0} \propto \xi \equiv \Omega_{\chi_1^0} h^2 / 0.11$.

- The higgsino scenario accounts for the upper band of relic density and scaled SI cross section in the corresponding panels in Fig. 7, and is therefore within reach of future detectors such as LUX or Xenon 1 Ton.
- A wino dominated χ_1^0 is more suppressed than the higgsino scenario, and resides in the lower band of the relic abundance and σ_{SI} and may fall beyond the reach of Xenon 1 Ton.

Since the primary exchange for σ_{SD} occurs through a Z boson, the cross section is proportional to the higgsino asymmetry. This asymmetry is generally suppressed for large neutralino masses. The current experimental sensitivity of COUPP is about an order of magnitude larger than the scaled scattering rate, $\xi \sigma_{\text{SD}}$. However, the sensitivity from IceCube does not critically depend on ξ . Therefore, for masses below 500 GeV, IceCube may soon be sensitive to both higgsino and wino scenarios.

C. Universal Extra Dimensions

In this section, we present updated results [220, 221] on the complementarity between high-energy colliders and dark matter direct detection experiments in the context of Universal Extra Dimensions [222]. As our reference, we take the mass spectrum in Minimal Universal Extra Dimensions (MUED), which is fixed by the radius (R) of the extra dimension and the cut-off scale (Λ) [223, 224]. To illustrate the complementarity between dark matter detection and searches at the LHC, we introduce a slope in the MUED mass spectrum, in terms of the mass splitting (Δ_{q_1}) between the mass of the lightest Kaluza-Klein (KK) partner (LKP) m_{LKP} and the KK quark mass m_{q_1} , $\Delta_{q_1} = \frac{m_{q_1} - m_{LKP}}{m_{LKP}}$. We take Δ_{q_1} as a free parameter, which is possible in a more general framework with boundary terms and bulk masses (see, e.g., [225]). The LKP is taken to be either the KK mode γ_1 of the photon (as in MUED), or the KK mode Z_1 of the Z -boson. In the latter case, we assume the gluon and the remaining particles to be respectively 20% and 10% heavier than the Z_1 . This choice is only made for definiteness, and does not impact our results, as long as the remaining particles are sufficiently heavy and do not participate in co-annihilation processes.

In the so defined (m_{LKP}, Δ_{q_1}) parameter plane, in Fig. 8 we superimpose the limit on the spin-independent elastic scattering cross section, the limit on the relic abundance and the LHC reach in the four leptons plus missing energy ($4\ell + \cancel{E}_T$) channel which has been studied in [223] at the 14 TeV (see Ref. [226] for 7+8 TeV). This signature results from the pair production (direct or indirect)

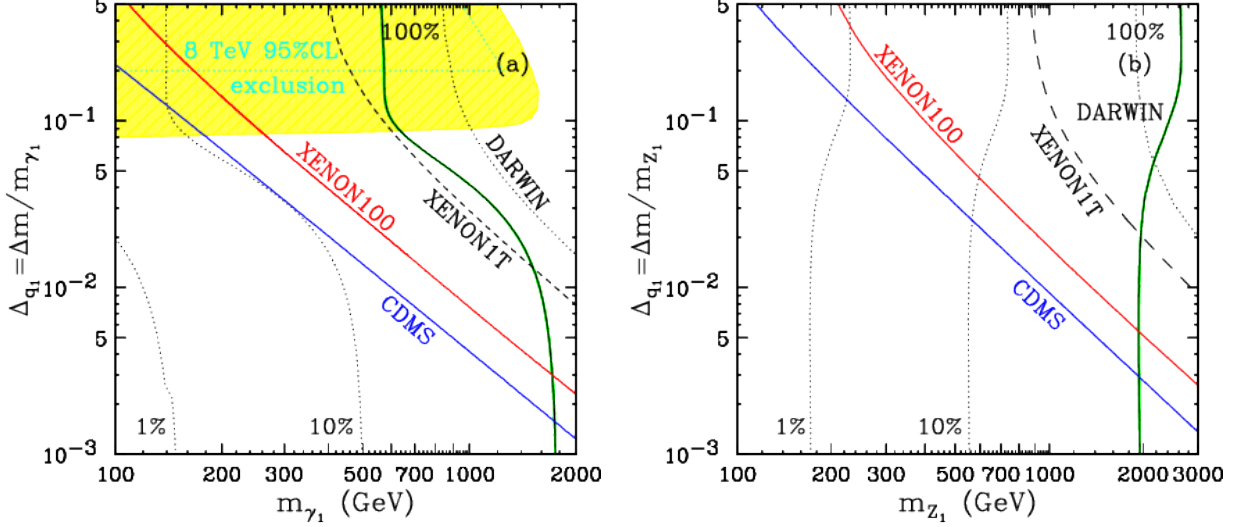


FIG. 8: Combined plot of the direct detection limit on the spin-independent cross section, the limit from the relic abundance and the LHC reach for (a) γ_1 and (b) Z_1 , in the parameter plane of the LKP mass and the mass splitting Δ_{q_1} . The remaining KK masses have been fixed as in Ref. [224] and the SM Higgs mass is $m_h = 125$ GeV. $\Lambda R = 20$ is assumed. The black solid line accounts for all of the dark matter (100%) and the two black dotted lines show 10% and 1%, respectively. The green band shows the WMAP/Planck range, $0.117 < \Omega_{CDM} h^2 < 0.1204$. The blue (red) solid line labelled by CDMS (XENON100) shows the current limit of the experiment whereas the dashed and dotted lines represent projected limits of future experiments. In the case of γ_1 LKP, a ton-scale experiment will rule out most of the parameter space while there is little parameter space left in the case of Z_1 LKP. The yellow region in the case of γ_1 LKP shows parameter space that could be covered by the collider search in the $4\ell + \cancel{E}_T$ channel at the LHC with a luminosity of 100 fb^{-1} [223]. (Figures taken from [221].)

of $SU(2)_W$ -doublet KK quarks, which subsequently decay to Z_1 's and jets. The leptons (electrons or muons) arise from the $Z_1 \rightarrow \ell^+ \ell^- \gamma_1$ decay, whose branching fraction is approximately $1/3$ [223]. Requiring a 5σ excess at a luminosity of 100 fb^{-1} , the LHC reach extends up to $R^{-1} \approx m_{\gamma_1} \sim 1.5$ TeV, which is shown as the right-most boundary of the (yellow) shaded region in Fig. 8a. The slope of that boundary is due to the fact that as Δ_{q_1} increases, so do the KK quark masses, and their production cross sections are correspondingly getting suppressed, diminishing the reach. We account for the loss in cross section according to the results from Ref. [227], assuming also that, as expected, the level-2 KK particles are about two times heavier than those at level 1. Points which are well inside the (yellow) shaded region, of course, would be discovered much earlier at the LHC. Notice, however, that the LHC reach in this channel completely disappears for Δ_{q_1} less than about 8%. This is where the KK quarks become lighter than the Z_1 (recall that in Fig. 8a m_{Z_1} is fixed according to the MUED spectrum) and the $q_1 \rightarrow Z_1$ decays are turned off. Instead, the KK quarks all decay directly to the γ_1 LKP and (relatively soft) jets, presenting a monumental challenge for an LHC discovery. So far there have been no studies of the collider phenomenology of a Z_1 LKP scenario, but it appears to be extremely challenging, especially if the KK quarks are light and decay directly to the LKP. This is why there is no LHC reach shown in Fig. 8b. We draw attention once again to the lack of sensitivity at small Δ_{q_1} : such small mass splittings are quite problematic for collider searches. The current LHC exclusion limit (95% C.L. at 8 TeV) on R^{-1} is about 1250 GeV for $\Lambda R = 20$ [226], and this is shown as the dotted (cyan) line. The horizontal line at $\Delta_{q_1} \sim 0.2$ is the average mass splitting in MUED. To indicate roughly the approximate boundary of the excluded region, the slanted line around 1 TeV is added, assuming the shape of the boundary is similar to that for the LHC14 reach.

In Fig. 8 we contrast the LHC reach with the relic density constraints [26, 228] and with the sensitivity of direct detection experiments [27, 229]. The green shaded region labelled by 100% represents the 2σ band, $0.117 < \Omega_{CDM}h^2 < 0.1204$ [230] and the black solid line inside this band is the central value $\Omega_{CDM}h^2 = 0.1187$. The region above and to the right of this band is disfavored since UED would then predict too much dark matter. The green-shaded region is where KK dark matter is sufficient to explain all of the dark matter in the universe, while in the remaining region to the left of the green band the LKP can make up only a fraction of the dark matter in the universe. We have indicated with the black dotted contours the parameter region where the LKP would contribute only 10% and 1% to the total dark matter budget. Finally, the solid (CDMS [231] in blue and XENON100 [181] in red) lines show the current direct detection limits, while the dotted and dashed lines show projected sensitivities for future experiments [207, 232, 233] (without rescaling by the calculated relic density).

Fig. 8 demonstrates the complementarity between the three different types of probes which we are considering. First, the parameter space region at very large m_{LKP} is inconsistent with cosmology – if the dark matter WIMP is too heavy, its relic density is too large. The exact numerical bound on the LKP mass may vary, depending on the particle nature of the WIMP (compare Fig. 8a to Fig. 8b) and the presence or absence of coannihilations (compare the m_{LKP} bound at small Δ_{q_1} to the bound at large Δ_{q_1}). Nevertheless, we can see that, in general, cosmology does provide an upper limit on the WIMP mass. On the other hand, colliders are sensitive to the region of relatively large mass splittings Δ_{q_1} , while direct detection experiments are at their best at small Δ_{q_1} and small m_{LKP} . The relevant parameter space is therefore getting squeezed from opposite directions and is bound to be covered eventually. This is already seen in the case of γ_1 LKP from Fig. 8a: the future experiments push up the current limit almost to the WMAP/Planck band. In the case of Z_1 LKP the available parameter space is larger and will not be closed with the currently envisioned experiments alone. However, one should keep in mind that detailed LHC studies for that scenario are still lacking.

Similarly the spin-dependent elastic scattering cross sections also exhibit an enhancement at small Δ_{q_1} . In Fig. 9 we combine existing limits from three different experiments (XENON100 [234], SIMPLE [235] and COUPP [219]) in the (m_{LKP}, Δ_{q_1}) plane. Panel (a) (panel (b)) shows the constraints from the WIMP-neutron (WIMP-proton) SD cross sections. The rest of the KK spectrum has been fixed as in Fig. 8. The solid (dashed) curves are limits on γ_1 (Z_1) from each experiment. The constraints from LHC and WMAP on the (m_{LKP}, Δ_{q_1}) parameter space are the same as in Fig. 8.

By comparing Figs. 8 and 9 we see that, as expected, the parameter space constraints for SI interactions are stronger than those for SD interactions. For example, in perhaps the most interesting range of LKP masses from 300 GeV to 1 TeV, the SI limits on Δ_{q_1} in Fig. 8 range from $\sim 10^{-1}$ down to $\sim 10^{-2}$. On the other hand, the SD bounds on Δ_{q_1} for the same range of m_{LKP} are about an order of magnitude smaller (i.e. weaker). We also notice that the constraints for γ_1 LKP are stronger than for Z_1 LKP. This can be easily understood since for the same LKP mass and KK mass splitting, the γ_1 SD cross sections are typically larger.

Fig. 9 also reveals that the experiments rank differently with respect to their SD limits on protons and neutrons. For example, SIMPLE and COUPP are more sensitive to the proton cross section, while XENON100 is more sensitive to the neutron cross section. As a result, the current best SD limit on protons comes from COUPP, but the current best SD limit on neutrons comes from XENON100.

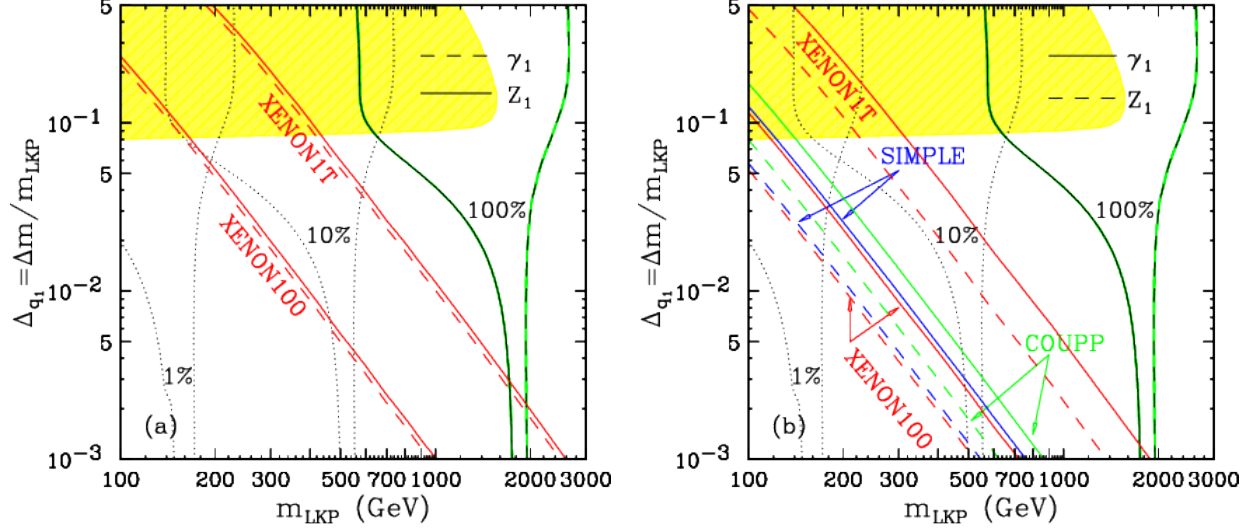


FIG. 9: Experimental upper bounds (90% C.L.) on the spin-dependent elastic scattering cross sections on (a) neutrons and (b) protons in the m_{LKP} - Δ_{q1} plane. The solid (dashed) curves are limits on γ_1 (Z_1) from each experiment. Shaded regions and dotted lines are defined in the same way as in Fig. 8. The depicted LHC reach (yellow shaded region) applies only to the case of γ_1 LKP. (Figures taken from [221].)

D. Self-interacting dark matter

In this section, we consider dark matter that has a large cross section for scattering off of itself. We will consider simple hidden sector models where such phenomenology is realized and show that they make rather concrete predictions for direct and indirect detection experiments. This provides a simple but concrete example of complementarity between astrophysics and direct or indirect searches. The basic premise here is that dark matter particles can have a large cross section for elastically scattering with other dark matter particles. It is also possible that a subdominant fraction of the dark matter particles interact through dissipative collisions [236]. The general scenario with collisional dark matter has been dubbed self-interacting DM (SIDM) [130, 237]. SIDM can affect the internal structure of DM halos (density profiles and shapes) compared to collisionless DM. In turn, astrophysical observations of structure formation, compared to N-body simulations, can probe the self-interacting nature of DM. It is worth emphasizing that tests of self-interactions can shed light on the nature of DM *even if DM is completely decoupled with respect to traditional DM searches*.

In fact, there are long-standing issues on small scales that may point toward SIDM. Dwarf galaxies are natural DM laboratories since in these galaxies DM tends to dominate baryons well inside the optical radius. Observations indicate that the central regions of well-resolved dwarf galaxies exhibit cored profiles [238, 239], as opposed to steeper cusp profiles found in collisionless DM-only simulations [240]. Cored profiles have been inferred in a variety of dwarf halos, including within the Milky Way (MW) [241], other nearby dwarfs [242] and low surface brightness galaxies [243]. An additional problem concerns the number of massive dwarf spheroidals in the MW. Collisionless DM simulations have a population of subhalos in MW-like halos that are too massive to host any of the known dwarf spheroidals but whose star formation should not have been suppressed by ultraviolet feedback [244]. While these apparent anomalies are not yet conclusive – e.g., baryonic feedback effects may be important [245] – recent state-of-the-art SIDM N-body simulations have shown that self-interactions can modify the properties of dwarf halos to be in accord with observations, without spoiling the success of collisionless DM on larger scales and being consistent with halo shape and

Bullet Cluster bounds [117, 131, 246, 247].

The figure of merit for DM self-interactions is cross section per unit DM mass, σ/m_χ , where χ is the DM particle. To have an observable effect on DM halos over cosmological timescales, the required cross section per unit mass must be³

$$\sigma/m_\chi \sim 1 \text{ cm}^2/\text{g} \approx 2 \text{ barns/GeV}, \quad (8)$$

or larger. From a particle physics perspective, this value is many orders of magnitude larger than the typical weak-scale cross section expected for a WIMP ($\sigma \sim 1$ picobarn). Evidence for self-interactions would therefore point toward a new dark mediator particle ϕ that is much lighter than the weak scale. Such light mediators have been invoked within a variety of other DM contexts as well, including explaining various indirect detection anomalies; see e.g. [88, 89, 249].

As one example, DM self-interactions can arise if DM is coupled to a massive dark photon ϕ from a hidden $U(1)'$ gauge symmetry [40, 76–79, 248, 250]. Other examples where dark matter self-interactions arise include mirror dark matter [251–253] and atomic dark matter [80, 254], both appearing in the framework of hidden sector dark matter. The non-relativistic self-scattering mediated by a dark photon can be described by a Yukawa potential,

$$V(r) = \pm \frac{\alpha_\chi}{r} e^{-m_\phi r}, \quad (9)$$

where α_χ is the “dark fine structure constant.” For symmetric DM (both $\chi, \bar{\chi}$ are present today) scattering can be repulsive (+) or attractive (−), while for asymmetric DM (only χ is present today) scattering is purely repulsive. Given the potential in Eq. (9), the cross section σ can be computed using standard methods from quantum mechanics as a function of the three parameters ($m_\chi, m_\phi, \alpha_\chi$) and the relative velocity v [248].

Different size DM halos have different characteristic velocities, giving complementary information about $\sigma(v)$. Similar to Rutherford scattering, DM self-scattering through a light mediator is typically suppressed at large velocities compared to smaller velocities. Therefore, it is natural for DM to be self-interacting in smaller dwarf halos, while appearing to be collisionless in larger halos. For example, the Bullet Cluster is often quoted as an example of an observation that categorically rules out self-interactions in the dark sector. This is not true since the relative velocity in the Bullet Cluster system ($v \approx 3000$ km/s) is much larger than in dwarf halos (30 km/s). As we show below, this constraint, while important, eliminates only a small region of SIDM parameter space.

Aside from self-interactions, the mediator ϕ can also set the DM relic density in the early Universe through $\chi\bar{\chi} \rightarrow \phi\phi$ annihilation. For symmetric DM, the required annihilation cross section is $\langle\sigma v\rangle_{\text{ann}} \approx 5 \times 10^{-26} \text{ cm}^3/\text{s}$, which fixes $\alpha_\chi \approx 4 \times 10^{-5} (m_\chi/\text{GeV})$. For asymmetric DM, although the relic density is determined by a primordial asymmetry, $\langle\sigma v\rangle_{\text{ann}}$ has to be *larger* than in the symmetric case, implying $\alpha_\chi \gtrsim 4 \times 10^{-5} (m_\chi/\text{GeV})$.

Fig. 10 shows the parameter space for this SIDM model as a function of m_χ and m_ϕ . The left panel corresponds to symmetric DM, where α_χ is fixed by relic density, while the right panel corresponds to asymmetric DM with $\alpha_\chi = 10^{-2}$. The shaded regions show where SIDM can explain halo anomalies on dwarf scales, with a generous range of cross section $0.1 \lesssim \sigma/m_\chi \lesssim 10 \text{ cm}^2/\text{s}$ and taking a characteristic velocity $v_0 = 30$ km/s. The contours labeled “SIDM” show where $\sigma/m_\chi = 0.1, 1, 10 \text{ cm}^2/\text{s}$ on dwarf scales. To implement the Bullet Cluster constraint, we require $\sigma/m_\chi \lesssim 1 \text{ cm}^2/\text{g}$ for a relative velocity $v \approx 3000$ km/s [132], shown by the green dot-dashed contour. Other constraints arise from the ellipticity of DM halos of galaxies; we require $\sigma/m_\chi \lesssim$

³ Here, σ refers to the momentum-transfer weighted cross section averaged over a Maxwellian velocity distribution for a given halo with characteristic (most probable) velocity v_0 . See Ref. [248] for further details.

FIG. 10: Parameter space for SIDM χ with a vector mediator ϕ , as a function of their masses m_χ, m_ϕ , for symmetric DM with α_χ fixed by relic density (left) and asymmetric DM with $\alpha_\chi = 10^{-2}$ (right). Shaded region indicates the region where DM self-interactions would lower densities in the central parts of dwarf scales consistent with observations. The upper (lower) boundary corresponds to $\langle\sigma_T\rangle/m_\chi = 0.1$ (10) cm^2/g . Dot-dashed curves show halo shape constraints on group scales ($\sigma/m_\chi < 1$ cm^2/g) and the Bullet Cluster constraint ($\sigma/m_\chi < 1$ cm^2/g). Dashed lines show direct detection sensitivity for XENON1T if ϕ has kinetic mixing with the photon with $\epsilon = 10^{-10}$. The vertical hatched boundary shows exclusion from CMB if $\phi \rightarrow e^+e^-$. See text for details.

1 cm^2/s for halos of characteristic velocity $v_0 \approx 300$ km/s [246], shown by the red dot-dashed contour (“Halo shapes”). From these bounds, the low (m_χ, m_ϕ) region is excluded in Fig. 10.

The dark and visible sectors need not be completely decoupled. For example, if there exist new states charged under both the Standard Model (SM) and $U(1)'$ gauge symmetries, mixing can arise between ϕ and the photon or Z boson. This generates effective couplings of ϕ to protons and neutrons, giving rise to signals in direct detection experiments. In the limit of zero momentum transfer, the spin-independent (SI) χ -nucleon cross section can be written as

$$\sigma_{\chi n}^{\text{SI}} = \frac{16\pi\alpha_\chi\alpha_{\text{em}}\epsilon_{\text{eff}}^2\mu_{\chi n}^2}{m_\phi^4} \approx 10^{-24} \text{ cm}^2 \times \epsilon_{\text{eff}}^2 \left(\frac{30 \text{ MeV}}{m_\phi} \right)^4 \times \begin{cases} (m_\chi/200 \text{ GeV}) & \text{symmetric DM} \\ (\alpha_\chi/10^{-2}) & \text{asymmetric DM} \end{cases}, \quad (10)$$

where $\mu_{\chi n}$ is the χ -nucleon reduced mass, α_{em} is the electromagnetic fine structure constant, and ϵ_{eff} is the effective ϕ -nucleon coupling, normalized to the proton electric charge e . Since SIDM prefers a very light mediator, with mass $m_\phi \sim 10 - 100$ MeV , it is clear that direct detection experiments, with current XENON100 limits approaching $\sigma_{\chi n}^{\text{SI}} \sim 10^{-45}$ [181], are sensitive to very small couplings ϵ_{eff} .

As an example, we consider the case of kinetic mixing between ϕ and the photon, governed by the parameter ϵ [85]. This mixing induces a coupling of ϕ to SM particles carrying electric charge, so that ϕ decays predominantly to e^+e^- for m_ϕ in the $10 - 100$ MeV range preferred for SIDM. The direct detection cross section is governed by the ϕ -proton coupling with $\epsilon_{\text{eff}} = \epsilon Z/A$, where Z/A is the proton fraction of the target nucleus. However, there are various constraints on the ϵ . Late decays of ϕ can inject energy to the plasma and modify standard big bang nucleosynthesis

FIG. 11: Prospects for direct detection of self-interacting DM that couples to quarks via gauge kinetic mixing with $\epsilon = 10^{-10}$. Left figure is for symmetric DM, with α_X fixed by relic density constraints; right figure is asymmetric DM, with $\alpha_X = 10^{-2}$. Shaded region indicates the region where DM self-interactions would lower densities in the central parts of dwarf scales consistent with observations. The upper (lower) boundary corresponds to $\langle\sigma_T\rangle/m_\chi = 10 \text{ cm}^2/\text{g}$ ($0.1 \text{ cm}^2/\text{g}$). Direct detection sensitivity from future XENON1T experiments shown by dashed curves. Astrophysical limits from halo shapes and the Bullet Cluster shown by dot-dashed lines. The range of m_ϕ, α_X values are shown by dotted lines. The vertical hatched boundary shows exclusion from CMB if $\phi \rightarrow e^+e^-$ (left). These figures are taken from Ref. [255].

in the early Universe. Requiring the ϕ lifetime to be longer than ~ 1 second for leptonic decay modes, we derive a lower bound $\epsilon \gtrsim 10^{-10} \sqrt{10 \text{ MeV}/m_\phi}$ [256]. The upper bound from the low energy beam dump experiments is $\epsilon \lesssim 10^{-7}$ for $m_\phi \lesssim 400 \text{ MeV}$ [257], while the region $10^{-10} \lesssim \epsilon \lesssim 10^{-7}$ is excluded for $m_\phi \lesssim 100 \text{ MeV}$ by energy loss arguments in supernovae [258] (although this constraint depends sensitively on assumptions about the temperature and size of the supernova core). Regardless, for what follows, we take $\epsilon = 10^{-10}$ as a benchmark point.

Since the mediator mass $m_\phi \sim 1 - 100 \text{ MeV}$ is comparable or less than the typical momentum transfer $q \sim 50 \text{ MeV}$ in nuclear recoils, nuclear recoil interactions for SIDM are momentum-dependent and cannot be approximated by a contact interaction [259, 260]. Here, we take a simplified approach by multiplying the total $q^2 = 0$ DM-nucleus cross section by a q^2 -dependent form factor: $\sigma_{\chi N}^{\text{SI}}(q^2) = \sigma_{\chi N}^{\text{SI}}(q^2 = 0)f(q^2)$, with $f(q^2) = m_\phi^4/(m_\phi^2 + q^2)^2$. We take a fixed value $q = 50 \text{ MeV}$ for Xenon and assume that the cross section limits quoted in the XENON experiment apply to $\sigma_{\chi N}^{\text{SI}}(q^2)$ directly. We have checked that our simple approximation can reproduce the XENON100 reanalysis in [261]. It is interesting to note that the current XENON100 [181] limits are not sensitive to our benchmark SIDM model with $\epsilon = 10^{-10}$ because of the suppression from $f(q^2)$. Future direct detection experiments, such as LUX [262], SuperCDMS [263], and XENON1T will offer great sensitivity to directly detect SIDM. In Fig. 10, we show how direct detection sensitivities from XENON1T [207] map onto SIDM parameter space for $\epsilon = 10^{-10}$ and $Z/A \approx 0.4$ (purple dashed contours).

For symmetric DM, residual annihilation can lead to additional reionization around the recombination epoch via $\chi\bar{\chi} \rightarrow \phi\phi \rightarrow e^+e^-e^+e^-$, which is constrained by CMB observations [112, 264]. For $\text{BR}(\phi \rightarrow e^+e^-) = 1$, symmetric SIDM is excluded for m_χ below $\sim 30 \text{ GeV}$ [265], as indicated

in Fig. 10 (left) with the horizontal orange line. For asymmetric DM, this constraint does not apply. (We also note that this bound is weakened if ϕ decays to neutrinos, which occurs if ϕ mixes with the Z boson.)

For symmetric dark matter there are further connections to indirect searches in the context of models with kinetic mixing. Annihilation to electrons and positrons locally will be constrained by the AMS-02 data [103], while Fermi Large Area Telescope will be sensitive to annihilation in the Galactic Center.

In Fig. 11, we illustrate the complementarity between astrophysical probes and direct detection in constraining SIDM. Fixing $\epsilon = 10^{-10}$, we show the SIDM prediction for SI scattering in direct detection experiments for both symmetric DM (left) and asymmetric DM (right). As in Fig. 10, the shaded band shows the preferred parameter region for solving dwarf-scale anomalies, while the red and green contours denote limits from halo shape observations and the Bullet Cluster, respectively. The purple dashed lines show the projected XENON1T bounds [207]. The dotted gray lines denote contours of constant α_χ and m_ϕ . This figure clearly demonstrates that astrophysical observations and direct detection experiments complement each other in the search for SIDM candidates.

VI. POST-DISCOVERY COMPLEMENTARITY

As important as a broad program of complementary searches is to establishing a compelling signal for dark matter, it becomes even more important after a signal has been reported for several reasons.

First, as is well known, many tentative dark matter signals have already been reported. The potential identification of a quarter of the Universe will require extraordinary proof in the form of verification by other experiments.

Second, each search strategy has its limitations. For example, as noted in Sec. IV, the discovery of a dark matter signal at particle colliders only establishes the production of a particle with lifetime greater than about 100 ns. The assumption that this particle contributes to dark matter requires an extrapolation in lifetime of 24 orders of magnitude! It is only by corroborating a particle collider discovery through another method that one can claim that the collider discovery is relevant for cosmology.

Last, the discovery of dark matter will usher in a rich and decades-long program of dark matter studies. Consider the following scenario: The LHC sees a missing energy signal, and precision measurements find evidence that it is due to a 60 GeV neutralino. This result is confirmed by direct search experiments, which discover a signal consistent with this mass. However, further LHC and ILC studies constrain the neutralino's predicted thermal relic density to be half of Ω_{DM} , implying that it is not a thermal relic, or that it makes up only half of the dark matter. The puzzle is resolved when axion detectors discover a signal, which is consistent with axions making up the rest of the dark matter, and progress in astrophysical theory, simulations, and observations leads to a consistent picture with dark matter composed entirely of CDM. The combined data establish a new standard cosmology in which dark matter is composed of equal parts neutralinos and axions, and extend our understanding of the early Universe back to neutralino freezeout, just 1 ns after the Big Bang. Direct and indirect detection rates are then used to constrain the local dark matter density, halo profiles, and substructure, establishing the new fields of neutralino and axion astronomy.

This two-component scenario is more complicated than assumed in many dark matter studies, but it is still relatively simple — as is often noted, the visible Universe has many components, and there is no reason that the dark Universe should be any simpler. As simple as this scenario is, however, it illustrates the point that, even for dark matter candidates that we have studied and

understood, the information provided by several approaches will be essential to understanding the particle nature of dark matter and its role in astrophysics and cosmology. A balanced program with components in each of the four approaches is required to cover the many well-motivated dark matter possibilities, and their interplay will likely be essential to realize the full potential of upcoming discoveries.

VII. CONCLUSIONS

The problem of identifying dark matter is central to the fields of particle physics and astrophysics, and has become a leading problem in all of basic science. In the coming decade, the field of dark matter will be transformed, with a perfect storm of experimental and technological progress set to put the most promising ideas to the test.

Dark matter searches rely on four approaches or pillars: direct detection, indirect detection, particle colliders, and astrophysical probes. In this Report, we have described the complementary relation of these approaches to each other. This complementarity may be seen on several levels. First, these approaches are qualitatively complementary: they differ in essential characteristics, and they rely on different dark matter properties to see a signal. A complementary set of approaches is required to be sensitive to the dark matter possibilities that are currently both viable and well-motivated. The approaches are also quantitatively complementary: within a given class of dark matter possibilities, these approaches are sensitive to different dark matter interactions and mass ranges.

Last, the discovery of a compelling dark matter signal is only the beginning. Complementary experiments are required to verify the initial discovery, to determine whether the particle makes up all of dark matter or only a portion, and to identify its essential properties, such as its interactions, spin, and mass, and to determine its role in forming the large scale structures of the Universe that we see today. A balanced dark matter program is required to carry out this research program to discover and study dark matter and to transform our understanding of the Universe on both the smallest and largest length scales.

Acknowledgements: MK would like to thank David Weinberg and Anze Slosar for input on section III D.

-
- [1] F. Zwicky, “Spectral displacement of extra galactic nebulae,” *Helv. Phys. Acta* **6** (1933) 110–127.
 - [2] V. C. Rubin and W. K. Ford, Jr., “Rotation of the Andromeda Nebula from a Spectroscopic Survey of Emission Regions,” *Astrophys. J.* **159** (1970) 379–403.
 - [3] V. C. Rubin, N. Thonnard, and W. K. Ford, Jr., “Rotational properties of 21 SC galaxies with a large range of luminosities and radii, from NGC 4605 ($R = 4$ kpc) to UGC 2885 ($R = 122$ kpc),” *Astrophys. J.* **238** (1980) 471.
 - [4] A. Bosma, *The distribution and kinematics of neutral hydrogen in spiral galaxies of various morphological types*. PhD thesis, PhD Thesis, Groningen Univ., (1978), 1978.
 - [5] A. Refregier, “Weak Gravitational Lensing by Large-Scale Structure,” *Ann. Rev. Astron. Astrophys.* **41** (2003) 645–668, [arXiv:astro-ph/0307212](#).
 - [6] J. A. Tyson, G. P. Kochanski, and I. P. Dell’Antonio, “Detailed Mass Map of CL0024+1654 from Strong Lensing,” *Astrophys. J.* **498** (1998) L107, [arXiv:astro-ph/9801193](#).
 - [7] A. D. Lewis, D. A. Buote, and J. T. Stocke, “Chandra Observations of Abell 2029: The Dark Matter Profile at $< 0.01R_{\text{vir}}$ in an Unusually Relaxed Cluster,” *Astrophys. J.* **586** (2003) 135–142, [arXiv:astro-ph/0209205](#).

- [8] S. W. Allen, A. C. Fabian, R. W. Schmidt, and H. Ebeling, “Cosmological constraints from the local X-ray luminosity function of the most X-ray luminous galaxy clusters,” *Mon. Not. Roy. Astron. Soc.* **342** (2003) 287, [arXiv:astro-ph/0208394](#).
- [9] D. Clowe *et al.*, “A direct empirical proof of the existence of dark matter,” *Astrophys. J.* **648** (2006) L109–L113, [arXiv:astro-ph/0608407](#).
- [10] **Particle Data Group** Collaboration, B. D. Fields and S. Sarkar, “Big Bang nucleosynthesis,” *Phys. Lett.* **B667** (2008) 228–231.
- [11] **Supernova Search Team** Collaboration, A. G. Riess *et al.*, “Observational Evidence from Supernovae for an Accelerating Universe and a Cosmological Constant,” *Astron. J.* **116** (1998) 1009–1038, [arXiv:astro-ph/9805201](#).
- [12] **Supernova Cosmology Project** Collaboration, S. Perlmutter *et al.*, “Measurements of Omega and Lambda from 42 High-Redshift Supernovae,” *Astrophys. J.* **517** (1999) 565–586, [arXiv:astro-ph/9812133](#).
- [13] **SDSS** Collaboration, M. Tegmark *et al.*, “Cosmological parameters from SDSS and WMAP,” *Phys.Rev.* **D69** (2004) 103501, [arXiv:astro-ph/0310723](#) [[astro-ph](#)].
- [14] E. Hawkins, S. Maddox, S. Cole, D. Madgwick, P. Norberg, *et al.*, “The 2dF Galaxy Redshift Survey: Correlation functions, peculiar velocities and the matter density of the universe,” *Mon.Not.Roy.Astron.Soc.* **346** (2003) 78, [arXiv:astro-ph/0212375](#) [[astro-ph](#)].
- [15] E. Komatsu *et al.*, “Seven-Year Wilkinson Microwave Anisotropy Probe (WMAP) Observations: Cosmological Interpretation,” [arXiv:1001.4538](#) [[astro-ph.CO](#)].
- [16] **Planck** Collaboration, P. Ade *et al.*, “Planck 2013 results. XVI. Cosmological parameters,” [arXiv:1303.5076](#) [[astro-ph.CO](#)].
- [17] G. Bertone, ed., *Particle Dark Matter: Observations, Models and Searches*. Cambridge University Press, 2010.
- [18] L. Bergstrom, “Dark Matter Candidates,” *New J.Phys.* **11** (2009) 105006, [arXiv:0903.4849](#) [[hep-ph](#)].
- [19] J. L. Feng, “Dark Matter Candidates from Particle Physics and Methods of Detection,” *Ann.Rev.Astron.Astrophys.* **48** (2010) 495–545, [arXiv:1003.0904](#) [[astro-ph.CO](#)].
- [20] Y. B. Zeldovich *Adv. Astron. Astrophys.* **3** (1965) 241.
- [21] H.-Y. Chiu, “Symmetry between particle and anti-particle populations in the universe,” *Phys. Rev. Lett.* **17** (1966) 712.
- [22] G. Steigman, “Cosmology Confronts Particle Physics,” *Ann. Rev. Nucl. Part. Sci.* **29** (1979) 313–338.
- [23] R. J. Scherrer and M. S. Turner, “On the Relic, Cosmic Abundance of Stable Weakly Interacting Massive Particles,” *Phys. Rev.* **D33** (1986) 1585.
- [24] H. Goldberg, “Constraint on the Photino Mass from Cosmology,” *Phys.Rev.Lett.* **50** (1983) 1419.
- [25] J. R. Ellis, J. Hagelin, D. V. Nanopoulos, K. A. Olive, and M. Srednicki, “Supersymmetric Relics from the Big Bang,” *Nucl.Phys.* **B238** (1984) 453–476.
- [26] G. Servant and T. M. Tait, “Is the lightest Kaluza-Klein particle a viable dark matter candidate?,” *Nucl.Phys.* **B650** (2003) 391–419, [arXiv:hep-ph/0206071](#) [[hep-ph](#)].
- [27] H.-C. Cheng, J. L. Feng, and K. T. Matchev, “Kaluza-Klein dark matter,” *Phys.Rev.Lett.* **89** (2002) 211301, [arXiv:hep-ph/0207125](#) [[hep-ph](#)].
- [28] K. Agashe and G. Servant, “Baryon number in warped GUTs: Model building and (dark matter related) phenomenology,” *JCAP* **0502** (2005) 002, [arXiv:hep-ph/0411254](#) [[hep-ph](#)].
- [29] J. Cembranos, A. Dobado, and A. L. Maroto, “Brane world dark matter,” *Phys.Rev.Lett.* **90** (2003) 241301, [arXiv:hep-ph/0302041](#) [[hep-ph](#)].
- [30] A. Birkedal-Hansen and J. G. Wacker, “Scalar dark matter from theory space,” *Phys.Rev.* **D69** (2004) 065022, [arXiv:hep-ph/0306161](#) [[hep-ph](#)].
- [31] H.-C. Cheng and I. Low, “TeV symmetry and the little hierarchy problem,” *JHEP* **0309** (2003) 051, [arXiv:hep-ph/0308199](#) [[hep-ph](#)].
- [32] L. Lopez Honorez, E. Nezri, J. F. Oliver, and M. H. Tytgat, “The Inert Doublet Model: An Archetype for Dark Matter,” *JCAP* **0702** (2007) 028, [arXiv:hep-ph/0612275](#) [[hep-ph](#)].
- [33] R. D. Peccei and H. R. Quinn, “Constraints Imposed by CP Conservation in the Presence of Instantons,” *Phys. Rev.* **D16** (1977) 1791–1797.
- [34] S. Weinberg, “A New Light Boson?,” *Phys. Rev. Lett.* **40** (1978) 223–226.

- [35] F. Wilczek, “Problem of Strong p and t Invariance in the Presence of Instantons,” *Phys. Rev. Lett.* **40** (1978) 279–282.
- [36] S. J. Asztalos, L. J. Rosenberg, K. van Bibber, P. Sikivie, and K. Zioutas, “Searches for astrophysical and cosmological axions,” *Ann.Rev.Nucl.Part.Sci.* **56** (2006) 293–326.
- [37] S. Dodelson and L. M. Widrow, “Sterile Neutrinos as Dark Matter,” *Phys. Rev. Lett.* **72** (1994) 17–20, [arXiv:hep-ph/9303287](#).
- [38] A. Kusenko, “Sterile neutrinos: the dark side of the light fermions,” *Phys. Rept.* **481** (2009) 1–28, [arXiv:0906.2968 \[hep-ph\]](#).
- [39] K. Abazajian, M. Acero, S. Agarwalla, A. Aguilar-Arevalo, C. Albright, *et al.*, “Light Sterile Neutrinos: A White Paper,” [arXiv:1204.5379 \[hep-ph\]](#).
- [40] J. L. Feng, M. Kaplinghat, H. Tu, and H.-B. Yu, “Hidden Charged Dark Matter,” *JCAP* **0907** (2009) 004, [arXiv:0905.3039 \[hep-ph\]](#).
- [41] D. E. Kaplan, G. Z. Krnjaic, K. R. Rehermann, and C. M. Wells, “Atomic Dark Matter,” *JCAP* **1005** (2010) 021, [arXiv:0909.0753 \[hep-ph\]](#).
- [42] S. Nussinov, “Technocosmology: Could a Technibaryon Excess Provide a ‘Natural’ Missing Mass Candidate?,” *Phys.Lett.* **B165** (1985) 55.
- [43] G. Gelmini, L. J. Hall, and M. Lin, “WHAT IS THE COSMION?,” *Nucl.Phys.* **B281** (1987) 726.
- [44] D. B. Kaplan, “A Single explanation for both the baryon and dark matter densities,” *Phys.Rev.Lett.* **68** (1992) 741–743.
- [45] S. M. Barr, “Baryogenesis, sphalerons and the cogeneration of dark matter,” *Phys.Rev.* **D44** (1991) 3062–3066.
- [46] D. E. Kaplan, M. A. Luty, and K. M. Zurek, “Asymmetric Dark Matter,” *Phys.Rev.* **D79** (2009) 115016, [arXiv:0901.4117 \[hep-ph\]](#).
- [47] L. Maiani *Proceedings: Summer School on Particle Physics, Paris, France* (1979) .
- [48] M. Veltman, “The Infrared - Ultraviolet Connection,” *Acta Phys.Polon.* **B12** (1981) 437.
- [49] E. Witten, “Dynamical Breaking of Supersymmetry,” *Nucl.Phys.* **B188** (1981) 513.
- [50] R. K. Kaul, “Gauge Hierarchy in a Supersymmetric Model,” *Phys.Lett.* **B109** (1982) 19.
- [51] S. Dimopoulos and H. Georgi, “Softly Broken Supersymmetry and SU(5),” *Nucl.Phys.* **B193** (1981) 150.
- [52] S. Dimopoulos, S. Raby, and F. Wilczek, “Supersymmetry and the Scale of Unification,” *Phys.Rev.* **D24** (1981) 1681–1683.
- [53] N. Sakai, “Naturalness in Supersymmetric Guts,” *Z.Phys.* **C11** (1981) 153.
- [54] L. E. Ibanez and G. G. Ross, “Low-Energy Predictions in Supersymmetric Grand Unified Theories,” *Phys.Lett.* **B105** (1981) 439.
- [55] M. Einhorn and D. Jones, “The Weak Mixing Angle and Unification Mass in Supersymmetric SU(5),” *Nucl.Phys.* **B196** (1982) 475.
- [56] K. Agashe and G. Servant, “Warped unification, proton stability and dark matter,” *Phys.Rev.Lett.* **93** (2004) 231805, [arXiv:hep-ph/0403143 \[hep-ph\]](#).
- [57] P. Sikivie, “Experimental Tests of the Invisible Axion,” *Phys.Rev.Lett.* **51** (1983) 1415.
- [58] H. Pagels and J. R. Primack, “Supersymmetry, Cosmology and New TeV Physics,” *Phys.Rev.Lett.* **48** (1982) 223.
- [59] S. Weinberg, “Cosmological Constraints on the Scale of Supersymmetry Breaking,” *Phys. Rev. Lett.* **48** (May, 1982) 1303–1306. <http://link.aps.org/doi/10.1103/PhysRevLett.48.1303>.
- [60] J. L. Feng, A. Rajaraman, and F. Takayama, “Superweakly interacting massive particles,” *Phys.Rev.Lett.* **91** (2003) 011302, [arXiv:hep-ph/0302215 \[hep-ph\]](#).
- [61] J. L. Feng, A. Rajaraman, and F. Takayama, “SuperWIMP dark matter signals from the early universe,” *Phys.Rev.* **D68** (2003) 063504, [arXiv:hep-ph/0306024 \[hep-ph\]](#).
- [62] S. M. Barr, R. S. Chivukula, and E. Farhi, “ELECTROWEAK FERMION NUMBER VIOLATION AND THE PRODUCTION OF STABLE PARTICLES IN THE EARLY UNIVERSE,” *Phys.Lett.* **B241** (1990) 387–391.
- [63] D. Hooper, J. March-Russell, and S. M. West, “Asymmetric sneutrino dark matter and the Omega(b) / Omega(DM) puzzle,” *Phys.Lett.* **B605** (2005) 228–236, [arXiv:hep-ph/0410114 \[hep-ph\]](#).
- [64] H. Davoudiasl and R. N. Mohapatra, “On Relating the Genesis of Cosmic Baryons and Dark Matter,” *New J.Phys.* **14** (2012) 095011, [arXiv:1203.1247 \[hep-ph\]](#).

- [65] K. Petraki and R. R. Volkas, “Review of asymmetric dark matter,” [arXiv:1305.4939 \[hep-ph\]](#).
- [66] S. D. McDermott, H.-B. Yu, and K. M. Zurek, “Constraints on Scalar Asymmetric Dark Matter from Black Hole Formation in Neutron Stars,” *Phys.Rev.* **D85** (2012) 023519, [arXiv:1103.5472 \[hep-ph\]](#).
- [67] C. Kouvaris and P. Tinyakov, “Excluding Light Asymmetric Bosonic Dark Matter,” *Phys.Rev.Lett.* **107** (2011) 091301, [arXiv:1104.0382 \[astro-ph.CO\]](#).
- [68] A. R. Zentner and A. P. Hearin, “Asymmetric Dark Matter May Alter the Evolution of Low-mass Stars and Brown Dwarfs,” *Phys.Rev.* **D84** (2011) 101302, [arXiv:1110.5919 \[astro-ph.CO\]](#).
- [69] F. Iocco, M. Taoso, F. Leclercq, and G. Meynet, “Main sequence stars with asymmetric dark matter,” *Phys.Rev.Lett.* **108** (2012) 061301, [arXiv:1201.5387 \[astro-ph.SR\]](#).
- [70] H. Davoudiasl, D. E. Morrissey, K. Sigurdson, and S. Tulin, “Hylogenesis: A Unified Origin for Baryonic Visible Matter and Antibaryonic Dark Matter,” *Phys.Rev.Lett.* **105** (2010) 211304, [arXiv:1008.2399 \[hep-ph\]](#).
- [71] T. Moroi and L. Randall, “Wino cold dark matter from anomaly mediated SUSY breaking,” *Nucl.Phys.* **B570** (2000) 455–472, [arXiv:hep-ph/9906527 \[hep-ph\]](#).
- [72] M. Fujii and K. Hamaguchi, “Nonthermal dark matter via Affleck-Dine baryogenesis and its detection possibility,” *Phys.Rev.* **D66** (2002) 083501, [arXiv:hep-ph/0205044 \[hep-ph\]](#).
- [73] R. Allahverdi, B. Dutta, and K. Sinha, “Successful Supersymmetric Dark Matter with Thermal Over/Under-Abundance from Late Decay of a Visible Sector Scalar,” *Phys.Rev.* **D87** (2013) 075024, [arXiv:1212.6948 \[hep-ph\]](#).
- [74] R. Allahverdi, M. Cicoli, B. Dutta, and K. Sinha, “Non-thermal Dark Matter in String Compactifications,” [arXiv:1307.5086 \[hep-ph\]](#).
- [75] J. L. Feng, H. Tu, and H.-B. Yu, “Thermal Relics in Hidden Sectors,” *JCAP* **0810** (2008) 043, [arXiv:0808.2318 \[hep-ph\]](#).
- [76] L. Ackerman, M. R. Buckley, S. M. Carroll, and M. Kamionkowski, “Dark Matter and Dark Radiation,” *Phys.Rev.* **D79** (2009) 023519, [arXiv:0810.5126 \[hep-ph\]](#).
- [77] J. L. Feng, M. Kaplinghat, and H.-B. Yu, “Halo Shape and Relic Density Exclusions of Sommerfeld-Enhanced Dark Matter Explanations of Cosmic Ray Excesses,” *Phys.Rev.Lett.* **104** (2010) 151301, [arXiv:0911.0422 \[hep-ph\]](#).
- [78] M. R. Buckley and P. J. Fox, “Dark Matter Self-Interactions and Light Force Carriers,” *Phys.Rev.* **D81** (2010) 083522, [arXiv:0911.3898 \[hep-ph\]](#).
- [79] A. Loeb and N. Weiner, “Cores in Dwarf Galaxies from Dark Matter with a Yukawa Potential,” *Phys.Rev.Lett.* **106** (2011) 171302, [arXiv:1011.6374 \[astro-ph.CO\]](#).
- [80] F.-Y. Cyr-Racine and K. Sigurdson, “The Cosmology of Atomic Dark Matter,” *Phys.Rev.* **D87** (2013) 103515, [arXiv:1209.5752 \[astro-ph.CO\]](#).
- [81] R. Foot, “Mirror matter-type dark matter,” *Int.J.Mod.Phys.* **D13** (2004) 2161–2192, [arXiv:astro-ph/0407623 \[astro-ph\]](#).
- [82] H. An, S.-L. Chen, R. N. Mohapatra, and Y. Zhang, “Leptogenesis as a Common Origin for Matter and Dark Matter,” *JHEP* **1003** (2010) 124, [arXiv:0911.4463 \[hep-ph\]](#).
- [83] J. Fan, A. Katz, L. Randall, and M. Reece, “Double-Disk Dark Matter,” [arXiv:1303.1521 \[astro-ph.CO\]](#).
- [84] B. Patt and F. Wilczek, “Higgs-field portal into hidden sectors,” [arXiv:hep-ph/0605188 \[hep-ph\]](#).
- [85] B. Holdom, “Two U(1)’s and Epsilon Charge Shifts,” *Phys.Lett.* **B166** (1986) 196.
- [86] D. Feldman, B. Kors, and P. Nath, “Extra-weakly Interacting Dark Matter,” *Phys.Rev.* **D75** (2007) 023503, [arXiv:hep-ph/0610133 \[hep-ph\]](#).
- [87] M. T. Frandsen, F. Kahlhoefer, S. Sarkar, and K. Schmidt-Hoberg, “Direct detection of dark matter in models with a light Z,” *JHEP* **1109** (2011) 128, [arXiv:1107.2118 \[hep-ph\]](#).
- [88] N. Arkani-Hamed, D. P. Finkbeiner, T. R. Slatyer, and N. Weiner, “A Theory of Dark Matter,” *Phys.Rev.* **D79** (2009) 015014, [arXiv:0810.0713 \[hep-ph\]](#).
- [89] M. Pospelov and A. Ritz, “Astrophysical Signatures of Secluded Dark Matter,” *Phys.Lett.* **B671** (2009) 391–397, [arXiv:0810.1502 \[hep-ph\]](#).
- [90] D. Feldman, Z. Liu, and P. Nath, “PAMELA Positron Excess as a Signal from the Hidden Sector,” *Phys.Rev.* **D79** (2009) 063509, [arXiv:0810.5762 \[hep-ph\]](#).
- [91] M. W. Goodman and E. Witten, “Detectability of Certain Dark Matter Candidates,” *Phys.Rev.* **D31** (1985) 3059.

- [92] “Table of Planned and Current Experiments.”
<http://www.snowmass2013.org/tiki-index.php?page=SLAC>.
- [93] “Indirect Detection Experiments.”
<http://www.snowmass2013.org/tiki-index.php?page=WIMP+Dark+Matter+Indirect+Detection>.
- [94] A. Geringer-Sameth and S. M. Koushiappas, “Exclusion of canonical WIMPs by the joint analysis of Milky Way dwarfs with Fermi,” *Phys.Rev.Lett.* **107** (2011) 241303, [arXiv:1108.2914](#) [[astro-ph.CO](#)].
- [95] **Fermi-LAT collaboration** Collaboration, M. Ackermann *et al.*, “Constraining Dark Matter Models from a Combined Analysis of Milky Way Satellites with the Fermi Large Area Telescope,” *Phys.Rev.Lett.* **107** (2011) 241302, [arXiv:1108.3546](#) [[astro-ph.HE](#)].
- [96] D. Hooper, C. Kelso, and F. S. Queiroz, “Stringent and Robust Constraints on the Dark Matter Annihilation Cross Section From the Region of the Galactic Center,” *Astropart.Phys.* **46** (2013) 55–70, [arXiv:1209.3015](#) [[astro-ph.HE](#)].
- [97] **H.E.S.S. Collaboration** Collaboration, A. Abramowski *et al.*, “Search for photon line-like signatures from Dark Matter annihilations with H.E.S.S.,” *Phys.Rev.Lett.* **110** (2013) 041301, [arXiv:1301.1173](#) [[astro-ph.HE](#)].
- [98] **HESS Collaboration** Collaboration, A. Abramowski *et al.*, “H.E.S.S. constraints on Dark Matter annihilations towards the Sculptor and Carina Dwarf Galaxies,” *Astropart.Phys.* **34** (2011) 608–616, [arXiv:1012.5602](#) [[astro-ph.HE](#)].
- [99] **Collaboration Alex Geringer-Sameth VERITAS** Collaboration, A. Geringer-Sameth, “The VERITAS Dark Matter Program,” [arXiv:1303.1406](#) [[astro-ph.HE](#)].
- [100] **VERITAS Collaboration** Collaboration, E. Aliu *et al.*, “VERITAS Deep Observations of the Dwarf Spheroidal Galaxy Segue 1,” *Phys.Rev.* **D85** (2012) 062001, [arXiv:1202.2144](#) [[astro-ph.HE](#)].
- [101] **MAGIC Collaboration** Collaboration, J. Aleksic *et al.*, “Searches for Dark Matter annihilation signatures in the Segue 1 satellite galaxy with the MAGIC-I telescope,” *JCAP* **1106** (2011) 035, [arXiv:1103.0477](#) [[astro-ph.HE](#)].
- [102] **PAMELA Collaboration** Collaboration, O. Adriani *et al.*, “An anomalous positron abundance in cosmic rays with energies 1.5-100 GeV,” *Nature* **458** (2009) 607–609, [arXiv:0810.4995](#) [[astro-ph](#)].
- [103] **AMS Collaboration** Collaboration, M. Aguilar *et al.*, “First Result from the Alpha Magnetic Spectrometer on the International Space Station: Precision Measurement of the Positron Fraction in Primary Cosmic Rays of 0.5350 GeV,” *Phys.Rev.Lett.* **110** no. 14, (2013) 141102.
- [104] D. Hooper, P. Blasi, and P. D. Serpico, “Pulsars as the Sources of High Energy Cosmic Ray Positrons,” *JCAP* **0901** (2009) 025, [arXiv:0810.1527](#) [[astro-ph](#)].
- [105] L. Bergstrom, T. Bringmann, I. Cholis, D. Hooper, and C. Weniger, “New limits on dark matter annihilation from AMS cosmic ray positron data,” *Phys.Rev.Lett.* (2013) , [arXiv:1306.3983](#) [[astro-ph.HE](#)].
- [106] **PAMELA Collaboration** Collaboration, O. Adriani *et al.*, “PAMELA results on the cosmic-ray antiproton flux from 60 MeV to 180 GeV in kinetic energy,” *Phys.Rev.Lett.* **105** (2010) 121101, [arXiv:1007.0821](#) [[astro-ph.HE](#)].
- [107] **IceCube collaboration** Collaboration, M. Aartsen *et al.*, “Search for dark matter annihilations in the Sun with the 79-string IceCube detector,” *Phys.Rev.Lett.* **110** (2013) 131302, [arXiv:1212.4097](#) [[astro-ph.HE](#)].
- [108] **CAST Collaboration** Collaboration, S. Aune *et al.*, “CAST search for sub-eV mass solar axions with ^3He buffer gas,” *Phys.Rev.Lett.* **107** (2011) 261302, [arXiv:1106.3919](#) [[hep-ex](#)].
- [109] N. Padmanabhan and D. P. Finkbeiner, “Detecting dark matter annihilation with CMB polarization: Signatures and experimental prospects,” *Phys.Rev.* **D72** (2005) 023508, [arXiv:astro-ph/0503486](#) [[astro-ph](#)].
- [110] M. Mapelli, A. Ferrara, and E. Pierpaoli, “Impact of dark matter decays and annihilations on reionization,” *Mon.Not.Roy.Astron.Soc.* **369** (2006) 1719–1724, [arXiv:astro-ph/0603237](#) [[astro-ph](#)].
- [111] L. Zhang, X.-L. Chen, Y.-A. Lei, and Z.-G. Si, “The impacts of dark matter particle annihilation on recombination and the anisotropies of the cosmic microwave background,” *Phys.Rev.* **D74** (2006) 103519, [arXiv:astro-ph/0603425](#) [[astro-ph](#)].
- [112] T. R. Slatyer, N. Padmanabhan, and D. P. Finkbeiner, “CMB Constraints on WIMP Annihilation:

- Energy Absorption During the Recombination Epoch,” *Phys.Rev.* **D80** (2009) 043526, [arXiv:0906.1197 \[astro-ph.CO\]](#).
- [113] “Energy Frontier Facilities List.” <http://www.snowmass2013.org/tiki-index.php?page=EF+Facilities+List>.
 - [114] D. H. Weinberg, J. S. Bullock, F. Governato, R. K. de Naray, and A. H. G. Peter, “Cold dark matter: controversies on small scales,” [arXiv:1306.0913 \[astro-ph.CO\]](#).
 - [115] A. A. Klypin, A. V. Kravtsov, O. Valenzuela, and F. Prada, “Where are the missing Galactic satellites?,” *Astrophys.J.* **522** (1999) 82–92, [arXiv:astro-ph/9901240 \[astro-ph\]](#).
 - [116] B. Moore, S. Ghigna, F. Governato, G. Lake, T. R. Quinn, *et al.*, “Dark matter substructure within galactic halos,” *Astrophys.J.* **524** (1999) L19–L22, [arXiv:astro-ph/9907411 \[astro-ph\]](#).
 - [117] M. Rocha, A. H. Peter, J. S. Bullock, M. Kaplinghat, S. Garrison-Kimmel, *et al.*, “Cosmological Simulations with Self-Interacting Dark Matter I: Constant Density Cores and Substructure,” [arXiv:1208.3025 \[astro-ph.CO\]](#).
 - [118] A. Kusenko, “Sterile neutrinos, dark matter, and the pulsar velocities in models with a Higgs singlet,” *Phys. Rev. Lett.* **97** (2006) 241301, [arXiv:hep-ph/0609081](#).
 - [119] **LSST Science Collaborations, LSST Project** Collaboration, P. A. Abell *et al.*, “LSST Science Book, Version 2.0,” [arXiv:0912.0201 \[astro-ph.IM\]](#).
 - [120] D. Spergel, N. Gehrels, J. Breckinridge, M. Donahue, A. Dressler, *et al.*, “Wide-Field InfraRed Survey Telescope-Astrophysics Focused Telescope Assets WFIRST-AFTA Final Report,” [arXiv:1305.5422 \[astro-ph.IM\]](#).
 - [121] R. Carlberg, C. Grillmair, and N. Hetherington, “The Pal 5 Star Stream Gaps,” *Astrophys.J.* **760** (2012) 75, [arXiv:1209.1741 \[astro-ph.CO\]](#).
 - [122] S. Vegetti, D. J. Lagattuta, J. P. McKean, M. W. Auger, C. D. Fassnacht, and L. V. E. Koopmans, “Gravitational detection of a low-mass dark satellite galaxy at cosmological distance,” *Nature (London)* **481** (Jan., 2012) 341–343, [arXiv:1201.3643 \[astro-ph.CO\]](#).
 - [123] L. A. Moustakas, K. Abazajian, A. Benson, A. S. Bolton, J. S. Bullock, *et al.*, “Strong gravitational lensing probes of the particle nature of dark matter,” [arXiv:0902.3219 \[astro-ph.CO\]](#).
 - [124] L. A. Moustakas, A. J. Bolton, J. T. Booth, J. S. Bullock, E. Cheng, *et al.*, “The Observatory for Multi-Epoch Gravitational Lens Astrophysics (OMEGA),” [arXiv:0806.1884 \[astro-ph\]](#).
 - [125] Y. Hezaveh, N. Dalal, G. Holder, M. Kuhlen, D. Marrone, *et al.*, “Dark Matter Substructure Detection Using Spatially Resolved Spectroscopy of Lensed Dusty Galaxies,” *Astrophys.J.* **767** (2013) 9, [arXiv:1210.4562 \[astro-ph.CO\]](#).
 - [126] U. Seljak, A. Makarov, P. McDonald, and H. Trac, “Can sterile neutrinos be the dark matter?,” *Phys.Rev.Lett.* **97** (2006) 191303, [arXiv:astro-ph/0602430 \[astro-ph\]](#).
 - [127] M. Viel, G. D. Becker, J. S. Bolton, and M. G. Haehnelt, “Warm Dark Matter as a solution to the small scale crisis: new constraints from high redshift Lyman-alpha forest data,” *Physical Review* **D88** no. 4, (2013) 043502, [arXiv:1306.2314 \[astro-ph.CO\]](#).
 - [128] M. Viel, J. Schaye, and C. M. Booth, “The impact of feedback from galaxy formation on the Lyman-alpha transmitted flux,” [arXiv:1207.6567 \[astro-ph.CO\]](#).
 - [129] N. Palanque-Delabrouille, C. Yche, A. Borde, J.-M. L. Goff, G. Rossi, *et al.*, “The one-dimensional Ly-alpha forest power spectrum from BOSS,” [arXiv:1306.5896 \[astro-ph.CO\]](#).
 - [130] D. N. Spergel and P. J. Steinhardt, “Observational evidence for selfinteracting cold dark matter,” *Phys.Rev.Lett.* **84** (2000) 3760–3763, [arXiv:astro-ph/9909386 \[astro-ph\]](#).
 - [131] M. Vogelsberger, J. Zavala, and A. Loeb, “Subhaloes in Self-Interacting Galactic Dark Matter Haloes,” *Mon.Not.Roy.Astron.Soc.* **423** (2012) 3740, [arXiv:1201.5892 \[astro-ph.CO\]](#).
 - [132] S. W. Randall, M. Markevitch, D. Clowe, A. H. Gonzalez, and M. Bradac, “Constraints on the Self-Interaction Cross-Section of Dark Matter from Numerical Simulations of the Merging Galaxy Cluster 1E 0657-56,” *Astrophys.J.* **679** (2008) 1173–1180, [arXiv:0704.0261 \[astro-ph\]](#).
 - [133] G. Raffelt, “Astrophysics probes of particle physics,” *Phys.Rept.* **333** (2000) 593–618.
 - [134] L. Zhang, X. Chen, M. Kamionkowski, Z.-g. Si, and Z. Zheng, “Constraints on radiative dark-matter decay from the cosmic microwave background,” *Phys.Rev.* **D76** (2007) 061301, [arXiv:0704.2444 \[astro-ph\]](#).
 - [135] J. Goodman, M. Ibe, A. Rajaraman, W. Shepherd, T. M. Tait, *et al.*, “Constraints on Light Majorana dark Matter from Colliders,” *Phys.Lett.* **B695** (2011) 185–188, [arXiv:1005.1286 \[hep-ph\]](#).

- [136] M. Beltran, D. Hooper, E. W. Kolb, Z. A. Krusberg, and T. M. Tait, “Maverick dark matter at colliders,” *JHEP* **1009** (2010) 037, [arXiv:1002.4137 \[hep-ph\]](#).
- [137] J. Goodman, M. Ibe, A. Rajaraman, W. Shepherd, T. M. Tait, *et al.*, “Constraints on Dark Matter from Colliders,” *Phys.Rev.* **D82** (2010) 116010, [arXiv:1008.1783 \[hep-ph\]](#).
- [138] Y. Bai, P. J. Fox, and R. Harnik, “The Tevatron at the Frontier of Dark Matter Direct Detection,” *JHEP* **1012** (2010) 048, [arXiv:1005.3797 \[hep-ph\]](#).
- [139] A. Rajaraman, W. Shepherd, T. M. Tait, and A. M. Wijangco, “LHC Bounds on Interactions of Dark Matter,” *Phys.Rev.* **D84** (2011) 095013, [arXiv:1108.1196 \[hep-ph\]](#).
- [140] P. J. Fox, R. Harnik, J. Kopp, and Y. Tsai, “Missing Energy Signatures of Dark Matter at the LHC,” *Phys.Rev.* **D85** (2012) 056011, [arXiv:1109.4398 \[hep-ph\]](#).
- [141] Y. Bai and T. M. Tait, “Searches with Mono-Leptons,” *Phys.Lett.* **B723** (2013) 384–387, [arXiv:1208.4361 \[hep-ph\]](#).
- [142] L. M. Carpenter, A. Nelson, C. Shimmmin, T. M. Tait, and D. Whiteson, “Collider searches for dark matter in events with a Z boson and missing energy,” [arXiv:1212.3352](#).
- [143] S. Profumo, W. Shepherd, and T. Tait, “The Pitfalls of Dark Crossings,” [arXiv:1307.6277 \[hep-ph\]](#).
- [144] M. T. Frandsen, F. Kahlhoefer, A. Preston, S. Sarkar, and K. Schmidt-Hoberg, “LHC and Tevatron Bounds on the Dark Matter Direct Detection Cross-Section for Vector Mediators,” *JHEP* **1207** (2012) 123, [arXiv:1204.3839 \[hep-ph\]](#).
- [145] H. An, X. Ji, and L.-T. Wang, “Light Dark Matter and Z' Dark Force at Colliders,” *JHEP* **1207** (2012) 182, [arXiv:1202.2894 \[hep-ph\]](#).
- [146] Y. Bai and J. Berger, “Fermion Portal Dark Matter,” [arXiv:1308.0612 \[hep-ph\]](#).
- [147] H. An, L.-T. Wang, and H. Zhang, “Dark matter with t -channel mediator: a simple step beyond contact interaction,” [arXiv:1308.0592 \[hep-ph\]](#).
- [148] S. Chang, R. Edezhath, J. Hutchinson, and M. Luty, “Effective WIMPs,” [arXiv:1307.8120 \[hep-ph\]](#).
- [149] A. DiFranzo, K. I. Nagao, A. Rajaraman, and T. M. P. Tait, “Simplified Models for Dark Matter Interacting with Quarks,” [arXiv:1308.2679 \[hep-ph\]](#).
- [150] G. Busoni, A. De Simone, E. Morgante, and A. Riotto, “On the Validity of the Effective Field Theory for Dark Matter Searches at the LHC,” [arXiv:1307.2253 \[hep-ph\]](#).
- [151] O. Buchmueller, M. J. Dolan, and C. McCabe, “Beyond Effective Field Theory for Dark Matter Searches at the LHC,” [arXiv:1308.6799 \[hep-ph\]](#).
- [152] “The Dark Matter Community Website.” <http://dmtools.brown.edu/>.
- [153] M. Wood, J. Buckley, S. Digel, S. Funk, D. Nieto, M. Sanchez-Conde, *et al.*, “CF2 White Paper: Prospects for Indirect Detection of Dark Matter with CTA.” http://www.snowmass2013.org/tiki-download_file.php?fileId=68.
- [154] **CMS** Collaboration, S. Chatrchyan *et al.*, “Search for dark matter and large extra dimensions in monojet events in pp collisions at $\sqrt{s} = 7$ TeV,” *JHEP* **1209** (2012) 094, [arXiv:1206.5663 \[hep-ex\]](#).
- [155] **ATLAS** Collaboration, G. Aad *et al.*, “Search for dark matter candidates and large extra dimensions in events with a jet and missing transverse momentum with the ATLAS detector,” [arXiv:1210.4491 \[hep-ex\]](#).
- [156] L. Vacavant and I. Hinchliffe, “Signals of models with large extra dimensions in ATLAS,” *J.Phys.* **G27** (2001) 1839–1850.
- [157] M. Beltran, D. Hooper, E. W. Kolb, and Z. C. Krusberg, “Deducing the nature of dark matter from direct and indirect detection experiments in the absence of collider signatures of new physics,” *Phys.Rev.* **D80** (2009) 043509, [arXiv:0808.3384 \[hep-ph\]](#).
- [158] P. J. Fox, R. Harnik, J. Kopp, and Y. Tsai, “LEP Shines Light on Dark Matter,” *Phys.Rev.* **D84** (2011) 014028, [arXiv:1103.0240 \[hep-ph\]](#).
- [159] Y. J. Chae and M. Perelstein, “Dark Matter Search at a Linear Collider: Effective Operator Approach,” [arXiv:1211.4008 \[hep-ph\]](#).
- [160] S. P. Martin, “A Supersymmetry primer,” [arXiv:hep-ph/9709356 \[hep-ph\]](#).
- [161] M. Cahill-Rowley, R. Cotta, A. Drlica-Wagner, S. Funk, J. Hewett, *et al.*, “Complementarity and Searches for Dark Matter in the pMSSM,” [arXiv:1305.6921 \[hep-ph\]](#).
- [162] C. F. Berger, J. S. Gainer, J. L. Hewett, and T. G. Rizzo, “Supersymmetry Without Prejudice,”

- JHEP* **0902** (2009) 023, [arXiv:0812.0980 \[hep-ph\]](#).
- [163] J. A. Conley, J. S. Gainer, J. L. Hewett, M. P. Le, and T. G. Rizzo, “Supersymmetry Without Prejudice at the LHC,” *Eur.Phys.J.* **C71** (2011) 1697, [arXiv:1009.2539 \[hep-ph\]](#).
 - [164] J. A. Conley, J. S. Gainer, J. L. Hewett, M. P. Le, and T. G. Rizzo, “Supersymmetry Without Prejudice at the 7 TeV LHC,” *Physical Review D* (2011) , [arXiv:1103.1697 \[hep-ph\]](#).
 - [165] M. W. Cahill-Rowley, J. L. Hewett, S. Hoeche, A. Ismail, and T. G. Rizzo, “The New Look pMSSM with Neutralino and Gravitino LSPs,” *Eur.Phys.J.* **C72** (2012) 2156, [arXiv:1206.4321 \[hep-ph\]](#).
 - [166] M. W. Cahill-Rowley, J. L. Hewett, A. Ismail, and T. G. Rizzo, “The Higgs Sector and Fine-Tuning in the pMSSM,” *Phys.Rev.* **D86** (2012) 075015, [arXiv:1206.5800 \[hep-ph\]](#).
 - [167] M. W. Cahill-Rowley, J. L. Hewett, A. Ismail, and T. G. Rizzo, “More Energy, More Searches, but the pMSSM Lives On,” [arXiv:1211.1981 \[hep-ph\]](#).
 - [168] B. Allanach, “SOFTSUSY: a program for calculating supersymmetric spectra,” *Comput.Phys.Commun.* **143** (2002) 305–331, [arXiv:hep-ph/0104145 \[hep-ph\]](#).
 - [169] A. Djouadi, J.-L. Kneur, and G. Moultaka, “SuSpect: A Fortran code for the supersymmetric and Higgs particle spectrum in the MSSM,” *Comput.Phys.Commun.* **176** (2007) 426–455, [arXiv:hep-ph/0211331 \[hep-ph\]](#).
 - [170] A. Djouadi, M. Muhlleitner, and M. Spira, “Decays of supersymmetric particles: The Program SUSY-HIT (SUspect-SdecaY-Hdecay-InTerface),” *Acta Phys.Polon.* **B38** (2007) 635–644, [arXiv:hep-ph/0609292 \[hep-ph\]](#).
 - [171] **ATLAS Collaboration** Collaboration, G. Aad *et al.*, “Observation of a new particle in the search for the Standard Model Higgs boson with the ATLAS detector at the LHC,” *Phys.Lett.* **B716** (2012) 1–29, [arXiv:1207.7214 \[hep-ex\]](#).
 - [172] **CMS Collaboration** Collaboration, S. Chatrchyan *et al.*, “Observation of a new boson at a mass of 125 GeV with the CMS experiment at the LHC,” *Phys.Lett.* **B716** (2012) 30–61, [arXiv:1207.7235 \[hep-ex\]](#).
 - [173] J. L. Feng and K. T. Matchev, “Focus point supersymmetry: Proton decay, flavor and CP violation, and the Higgs boson mass,” *Phys.Rev.* **D63** (2001) 095003, [arXiv:hep-ph/0011356 \[hep-ph\]](#).
 - [174] J. L. Feng, K. T. Matchev, and T. Moroi, “Multi - TeV scalars are natural in minimal supergravity,” *Phys.Rev.Lett.* **84** (2000) 2322–2325, [arXiv:hep-ph/9908309 \[hep-ph\]](#).
 - [175] J. L. Feng, K. T. Matchev, and T. Moroi, “Focus points and naturalness in supersymmetry,” *Phys.Rev.* **D61** (2000) 075005, [arXiv:hep-ph/9909334 \[hep-ph\]](#).
 - [176] J. L. Feng and D. Sanford, “A Natural 125 GeV Higgs Boson in the MSSM from Focus Point Supersymmetry with A-Terms,” *Phys.Rev.* **D86** (2012) 055015, [arXiv:1205.2372 \[hep-ph\]](#).
 - [177] J. L. Feng, K. T. Matchev, and F. Wilczek, “Neutralino dark matter in focus point supersymmetry,” *Phys.Lett.* **B482** (2000) 388–399, [arXiv:hep-ph/0004043 \[hep-ph\]](#).
 - [178] J. L. Feng, K. T. Matchev, and F. Wilczek, “Prospects for indirect detection of neutralino dark matter,” *Phys.Rev.* **D63** (2001) 045024, [arXiv:astro-ph/0008115 \[astro-ph\]](#).
 - [179] J. L. Feng and D. Sanford, “Heart of Darkness: The Significance of the Zeptobarn Scale for Neutralino Direct Detection,” *JCAP* **1105** (2011) 018, [arXiv:1009.3934 \[hep-ph\]](#).
 - [180] **ATLAS Collaboration** Collaboration, “Search for squarks and gluinos with the ATLAS detector using final states with jets and missing transverse momentum and 5.8 fb^{-1} of $\sqrt{s}=8 \text{ TeV}$ proton-proton collision data,”.
 - [181] **XENON100 Collaboration** Collaboration, E. Aprile *et al.*, “Dark Matter Results from 225 Live Days of XENON100 Data,” *Phys.Rev.Lett.* **109** (2012) 181301, [arXiv:1207.5988 \[astro-ph.CO\]](#).
 - [182] **COUPP Collaboration** Collaboration, E. Ramberg, “Developing a 60-kg bubble chamber for dark matter detection,” *Nucl.Instrum.Meth.* **A623** (2010) 454–456.
 - [183] **LAT Collaboration** Collaboration, W. Atwood *et al.*, “The Large Area Telescope on the Fermi Gamma-ray Space Telescope Mission,” *Astrophys.J.* **697** (2009) 1071–1102, [arXiv:0902.1089 \[astro-ph.IM\]](#).
 - [184] R. Harlander, P. Kant, L. Mihaila, and M. Steinhauser, “Higgs boson mass in supersymmetry to three loops,” *Phys.Rev.Lett.* **100** (2008) 191602, [arXiv:0803.0672 \[hep-ph\]](#).
 - [185] P. Kant, R. Harlander, L. Mihaila, and M. Steinhauser, “Light MSSM Higgs boson mass to three-loop accuracy,” *JHEP* **1008** (2010) 104, [arXiv:1005.5709 \[hep-ph\]](#).
 - [186] P. Draper, J. Feng, P. Kant, S. Profumo, and D. Sanford, “Dark Matter Detection in Focus Point Supersymmetry,” [arXiv:1304.1159 \[hep-ph\]](#).

- [187] J. L. Feng, K. T. Matchev, and D. Sanford, “Focus Point Supersymmetry Redux,” *Phys.Rev.* **D85** (2012) 075007, [arXiv:1112.3021 \[hep-ph\]](#).
- [188] G. Belanger, F. Boudjema, P. Brun, A. Pukhov, S. Rosier-Lees, *et al.*, “Indirect search for dark matter with micrOMEGAs2.4,” *Comput.Phys.Commun.* **182** (2011) 842–856, [arXiv:1004.1092 \[hep-ph\]](#).
- [189] P. Gondolo, J. Edsjo, P. Ullio, L. Bergstrom, M. Schelke, *et al.*, “DarkSUSY: Computing supersymmetric dark matter properties numerically,” *JCAP* **0407** (2004) 008, [arXiv:astro-ph/0406204 \[astro-ph\]](#).
- [190] W. Freeman and D. Toussaint, “The Strange quark content of the nucleon in 2+1 flavor lattice QCD,” *PoS LAT2009* (2009) 137, [arXiv:0912.1144 \[hep-lat\]](#).
- [191] R. Young and A. Thomas, “Octet baryon masses and sigma terms from an SU(3) chiral extrapolation,” *Phys.Rev.* **D81** (2010) 014503, [arXiv:0901.3310 \[hep-lat\]](#).
- [192] J. Giedt, A. W. Thomas, and R. D. Young, “Dark matter, the CMSSM and lattice QCD,” *Phys.Rev.Lett.* **103** (2009) 201802, [arXiv:0907.4177 \[hep-ph\]](#).
- [193] J. L. Feng, P. Kant, S. Profumo, and D. Sanford, “3-Loop Corrections to the Higgs Boson Mass and Implications for Supersymmetry at the LHC,” [arXiv:1306.2318 \[hep-ph\]](#).
- [194] H. Baer, V. Barger, P. Huang, A. Mustafayev, and X. Tata, “Radiative natural SUSY with a 125 GeV Higgs boson,” *Phys.Rev.Lett.* **109** (2012) 161802, [arXiv:1207.3343 \[hep-ph\]](#).
- [195] H. Baer, V. Barger, P. Huang, D. Mickelson, A. Mustafayev, *et al.*, “Radiative natural supersymmetry: Reconciling electroweak fine-tuning and the Higgs boson mass,” [arXiv:1212.2655 \[hep-ph\]](#).
- [196] H. Baer, V. Barger, P. Huang, D. Mickelson, A. Mustafayev, *et al.*, “Naturalness, Supersymmetry and Light Higgsinos: A Snowmass Whitepaper,” [arXiv:1306.2926 \[hep-ph\]](#).
- [197] A. G. Cohen, D. Kaplan, and A. Nelson, “The More minimal supersymmetric standard model,” *Phys.Lett.* **B388** (1996) 588–598, [arXiv:hep-ph/9607394 \[hep-ph\]](#).
- [198] T. Falk, “Higgsinos in SUSY models with gaugino mass unification,” *Phys.Lett.* **B456** (1999) 171–178, [arXiv:hep-ph/9902352 \[hep-ph\]](#).
- [199] J. Bagger, J. L. Feng, and N. Polonsky, “Naturally heavy scalars in supersymmetric grand unified theories,” *Nucl.Phys.* **B563** (1999) 3–20, [arXiv:hep-ph/9905292 \[hep-ph\]](#).
- [200] J. R. Ellis, K. A. Olive, and Y. Santoso, “The MSSM parameter space with nonuniversal Higgs masses,” *Phys.Lett.* **B539** (2002) 107–118, [arXiv:hep-ph/0204192 \[hep-ph\]](#).
- [201] H. Baer, V. Barger, and D. Mickelson, “Direct and indirect detection of higgsino-like WIMPs: concluding the story of electroweak naturalness,” [arXiv:1303.3816 \[hep-ph\]](#).
- [202] K.-Y. Choi, J. E. Kim, H. M. Lee, and O. Seto, “Neutralino dark matter from heavy axino decay,” *Phys.Rev.* **D77** (2008) 123501, [arXiv:0801.0491 \[hep-ph\]](#).
- [203] H. Baer, A. Lessa, S. Rajagopalan, and W. Sreethawong, “Mixed axion/neutralino cold dark matter in supersymmetric models,” *JCAP* **1106** (2011) 031, [arXiv:1103.5413 \[hep-ph\]](#).
- [204] H. Baer, A. Lessa, and W. Sreethawong, “Coupled Boltzmann calculation of mixed axion/neutralino cold dark matter production in the early universe,” *JCAP* **1201** (2012) 036, [arXiv:1110.2491 \[hep-ph\]](#).
- [205] K. J. Bae, H. Baer, and A. Lessa, “Dark Radiation Constraints on Mixed Axion/Neutralino Dark Matter,” *JCAP* **1304** (2013) 041, [arXiv:1301.7428 \[hep-ph\]](#).
- [206] A. Bottino, F. Donato, N. Fornengo, and S. Scopel, “Probing the supersymmetric parameter space by WIMP direct detection,” *Phys.Rev.* **D63** (2001) 125003, [arXiv:hep-ph/0010203 \[hep-ph\]](#).
- [207] **XENON1T collaboration** Collaboration, E. Aprile, “The XENON1T Dark Matter Search Experiment,” [arXiv:1206.6288 \[astro-ph.IM\]](#).
- [208] V. Barger, P. Langacker, and H.-S. Lee, “Lightest neutralino in extensions of the MSSM,” *Phys.Lett.* **B630** (2005) 85–99, [arXiv:hep-ph/0508027 \[hep-ph\]](#).
- [209] V. Barger, P. Langacker, I. Lewis, M. McCaskey, G. Shaughnessy, *et al.*, “Recoil Detection of the Lightest Neutralino in MSSM Singlet Extensions,” *Phys.Rev.* **D75** (2007) 115002, [arXiv:hep-ph/0702036 \[HEP-PH\]](#).
- [210] A. Djouadi, M. Drees, U. Ellwanger, R. Godbole, C. Hugonie, *et al.*, “Benchmark scenarios for the NMSSM,” *JHEP* **0807** (2008) 002, [arXiv:0801.4321 \[hep-ph\]](#).
- [211] U. Ellwanger, J. F. Gunion, and C. Hugonie, “NMHDECAY: A Fortran code for the Higgs masses, couplings and decay widths in the NMSSM,” *JHEP* **0502** (2005) 066, [arXiv:hep-ph/0406215](#)

- [hep-ph].
- [212] G. Belanger, F. Boudjema, A. Pukhov, and A. Semenov, “Dark matter direct detection rate in a generic model with micrOMEGAs 2.2,” *Comput.Phys.Commun.* **180** (2009) 747–767, [arXiv:0803.2360 \[hep-ph\]](#).
 - [213] **ATLAS Collaboration** Collaboration, “Search for direct production of charginos and neutralinos in events with three leptons and missing transverse momentum in 21 fb⁻¹ of pp collisions at $\sqrt{s} = 8$ TeV with the ATLAS detector,”.
 - [214] **ATLAS Collaboration** Collaboration, “Combined coupling measurements of the Higgs-like boson with the ATLAS detector using up to 25 fb⁻¹ of proton-proton collision data,”.
 - [215] **CMS Collaboration** Collaboration, “Combination of standard model Higgs boson searches and measurements of the properties of the new boson with a mass near 125 GeV,”.
 - [216] **LUX Collaboration** Collaboration, D. Akerib *et al.*, “Technical Results from the Surface Run of the LUX Dark Matter Experiment,” *Astropart.Phys.* **45** (2013) 34–43, [arXiv:1210.4569 \[astro-ph.IM\]](#).
 - [217] **IceCube Collaboration** Collaboration, R. Abbasi *et al.*, “Multi-year search for dark matter annihilations in the Sun with the AMANDA-II and IceCube detectors,” *Phys.Rev.* **D85** (2012) 042002, [arXiv:1112.1840 \[astro-ph.HE\]](#).
 - [218] M. McCaskey and G. Shaughnessy, “The NMSSM at the Cosmic Frontier for Snowmass 2013,” [arXiv:1307.0851 \[hep-ph\]](#).
 - [219] **COUPP Collaboration** Collaboration, E. Behnke *et al.*, “First Dark Matter Search Results from a 4-kg CF₃I Bubble Chamber Operated in a Deep Underground Site,” *Phys.Rev.* **D86** (2012) 052001, [arXiv:1204.3094 \[astro-ph.CO\]](#).
 - [220] S. Arrenberg, L. Baudis, K. Kong, K. T. Matchev, and J. Yoo, “Kaluza-Klein Dark Matter: Direct Detection vis-a-vis LHC,” *Phys.Rev.* **D78** (2008) 056002, [arXiv:0805.4210 \[hep-ph\]](#).
 - [221] S. Arrenberg, L. Baudis, K. Kong, K. T. Matchev, and J. Yoo, “Kaluza-Klein Dark Matter: Direct Detection vis-a-vis LHC (2013 update),” [arXiv:1307.6581 \[hep-ph\]](#).
 - [222] T. Appelquist, H.-C. Cheng, and B. A. Dobrescu, “Bounds on universal extra dimensions,” *Phys.Rev.* **D64** (2001) 035002, [arXiv:hep-ph/0012100 \[hep-ph\]](#).
 - [223] H.-C. Cheng, K. T. Matchev, and M. Schmaltz, “Bosonic supersymmetry? Getting fooled at the CERN LHC,” *Phys.Rev.* **D66** (2002) 056006, [arXiv:hep-ph/0205314 \[hep-ph\]](#).
 - [224] H.-C. Cheng, K. T. Matchev, and M. Schmaltz, “Radiative corrections to Kaluza-Klein masses,” *Phys.Rev.* **D66** (2002) 036005, [arXiv:hep-ph/0204342 \[hep-ph\]](#).
 - [225] T. Flacke, K. Kong, and S. C. Park, “Phenomenology of Universal Extra Dimensions with Bulk-Masses and Brane-Localized Terms,” *JHEP* **1305** (2013) 111, [arXiv:1303.0872 \[hep-ph\]](#).
 - [226] A. Belyaev, M. Brown, J. Moreno, and C. Papineau, “Discovering Minimal Universal Extra Dimensions (MUED) at the LHC,” *JHEP* **1306** (2013) 080, [arXiv:1212.4858 \[hep-ph\]](#).
 - [227] A. Datta, K. Kong, and K. T. Matchev, “Discrimination of supersymmetry and universal extra dimensions at hadron colliders,” *Phys.Rev.* **D72** (2005) 096006, [arXiv:hep-ph/0509246 \[hep-ph\]](#).
 - [228] K. Kong and K. T. Matchev, “Precise calculation of the relic density of Kaluza-Klein dark matter in universal extra dimensions,” *JHEP* **0601** (2006) 038, [arXiv:hep-ph/0509119 \[hep-ph\]](#).
 - [229] G. Servant and T. M. Tait, “Elastic scattering and direct detection of Kaluza-Klein dark matter,” *New J.Phys.* **4** (2002) 99, [arXiv:hep-ph/0209262 \[hep-ph\]](#).
 - [230] **Planck Collaboration** Collaboration, P. Ade *et al.*, “Planck 2013 results. XVI. Cosmological parameters,” [arXiv:1303.5076 \[astro-ph.CO\]](#).
 - [231] **CDMS-II Collaboration** Collaboration, Z. Ahmed *et al.*, “Dark Matter Search Results from the CDMS II Experiment,” *Science* **327** (2010) 1619–1621, [arXiv:0912.3592 \[astro-ph.CO\]](#).
 - [232] **DARWIN Consortium** Collaboration, L. Baudis, “DARWIN: dark matter WIMP search with noble liquids,” *J.Phys.Conf.Ser.* **375** (2012) 012028, [arXiv:1201.2402 \[astro-ph.IM\]](#).
 - [233] L. Baudis, “DARWIN: dark matter WIMP search with noble liquids,” *PoS IDM2010* (2011) 122, [arXiv:1012.4764 \[astro-ph.IM\]](#).
 - [234] **XENON100 Collaboration** Collaboration, E. Aprile *et al.*, “Limits on spin-dependent WIMP-nucleon cross sections from 225 live days of XENON100 data,” [arXiv:1301.6620 \[astro-ph.CO\]](#).
 - [235] M. Felizardo, T. Girard, T. Morlat, A. Fernandes, A. Ramos, *et al.*, “Final Analysis and Results of the Phase II SIMPLE Dark Matter Search,” *Phys.Rev.Lett.* **108** (2012) 201302, [arXiv:1106.3014](#)

- [astro-ph.CO].
- [236] J. Fan, A. Katz, L. Randall, and M. Reece, “A Dark-Disk Universe,” *Phys.Rev.Lett.* **110** (2013) 211302, [arXiv:1303.3271](#) [hep-ph].
 - [237] E. D. Carlson, M. E. Machacek, and L. J. Hall, “Self-interacting dark matter,” *Astrophys. J.* **398** (Oct., 1992) 43–52.
 - [238] B. Moore, “Evidence against dissipationless dark matter from observations of galaxy haloes,” *Nature* **370** (1994) 629.
 - [239] R. A. Flores and J. R. Primack, “Observational and theoretical constraints on singular dark matter halos,” *Astrophys.J.* **427** (1994) L1–4, [arXiv:astro-ph/9402004](#) [astro-ph].
 - [240] J. F. Navarro, C. S. Frenk, and S. D. White, “A Universal density profile from hierarchical clustering,” *Astrophys.J.* **490** (1997) 493–508, [arXiv:astro-ph/9611107](#) [astro-ph].
 - [241] M. G. Walker and J. Penarrubia, “A Method for Measuring (Slopes of) the Mass Profiles of Dwarf Spheroidal Galaxies,” *Astrophys.J.* **742** (2011) 20, [arXiv:1108.2404](#) [astro-ph.CO].
 - [242] S.-H. Oh, W. J. G. de Blok, E. Brinks, F. Walter, and R. C. Kennicutt, Jr., “Dark and Luminous Matter in THINGS Dwarf Galaxies,” *Astrophys.J.* **141** (June, 2011) 193, [arXiv:1011.0899](#) [astro-ph.CO].
 - [243] R. Kuzio de Naray, S. S. McGaugh, and W. J. G. de Blok, “Mass Models for Low Surface Brightness Galaxies with High-Resolution Optical Velocity Fields,” *Astrophys.J.* **676** (Apr., 2008) 920–943, [arXiv:0712.0860](#).
 - [244] M. Boylan-Kolchin, J. S. Bullock, and M. Kaplinghat, “The Milky Way’s bright satellites as an apparent failure of LCDM,” *Mon.Not.Roy.Astron.Soc.* **422** (2012) 1203–1218, [arXiv:1111.2048](#) [astro-ph.CO].
 - [245] F. Governato, A. Zolotov, A. Pontzen, C. Christensen, S. Oh, *et al.*, “Cuspy No More: How Outflows Affect the Central Dark Matter and Baryon Distribution in Lambda CDM Galaxies,” *Mon.Not.Roy.Astron.Soc.* **422** (2012) 1231–1240, [arXiv:1202.0554](#) [astro-ph.CO].
 - [246] A. H. Peter, M. Rocha, J. S. Bullock, and M. Kaplinghat, “Cosmological Simulations with Self-Interacting Dark Matter II: Halo Shapes vs. Observations,” [arXiv:1208.3026](#) [astro-ph.CO].
 - [247] J. Zavala, M. Vogelsberger, and M. G. Walker, “Constraining Self-Interacting Dark Matter with the Milky Way’s dwarf spheroidals,” [arXiv:1211.6426](#) [astro-ph.CO].
 - [248] S. Tulin, H.-B. Yu, and K. M. Zurek, “Beyond Collisionless Dark Matter: Particle Physics Dynamics for Dark Matter Halo Structure,” [arXiv:1302.3898](#) [hep-ph].
 - [249] J. L. Feng and J. Kumar, “The WIMPless Miracle: Dark-Matter Particles without Weak-Scale Masses or Weak Interactions,” *Phys.Rev.Lett.* **101** (2008) 231301, [arXiv:0803.4196](#) [hep-ph].
 - [250] S. Tulin, H.-B. Yu, and K. M. Zurek, “Resonant Dark Forces and Small Scale Structure,” [arXiv:1210.0900](#) [hep-ph].
 - [251] R. Mohapatra, S. Nussinov, and V. Teplitz, “Mirror matter as selfinteracting dark matter,” *Phys.Rev.* **D66** (2002) 063002, [arXiv:hep-ph/0111381](#) [hep-ph].
 - [252] R. Foot and R. Volkas, “Spheroidal galactic halos and mirror dark matter,” *Phys.Rev.* **D70** (2004) 123508, [arXiv:astro-ph/0407522](#) [astro-ph].
 - [253] R. Foot, “Implications of mirror dark matter kinetic mixing for CMB anisotropies,” *Phys.Lett.* **B718** (2013) 745–751, [arXiv:1208.6022](#) [astro-ph.CO].
 - [254] D. E. Kaplan, G. Z. Krnjaic, K. R. Rehermann, and C. M. Wells, “Dark Atoms: Asymmetry and Direct Detection,” *JCAP* **1110** (2011) 011, [arXiv:1105.2073](#) [hep-ph].
 - [255] M. Kaplinghat, S. Tulin, and H.-B. Yu, “Self-interacting Dark Matter Benchmarks,” [arXiv:1308.0618](#) [hep-ph].
 - [256] T. Lin, H.-B. Yu, and K. M. Zurek, “On Symmetric and Asymmetric Light Dark Matter,” *Phys.Rev.* **D85** (2012) 063503, [arXiv:1111.0293](#) [hep-ph].
 - [257] J. D. Bjorken, R. Essig, P. Schuster, and N. Toro, “New Fixed-Target Experiments to Search for Dark Gauge Forces,” *Phys.Rev.* **D80** (2009) 075018, [arXiv:0906.0580](#) [hep-ph].
 - [258] J. B. Dent, F. Ferrer, and L. M. Krauss, “Constraints on Light Hidden Sector Gauge Bosons from Supernova Cooling,” [arXiv:1201.2683](#) [astro-ph.CO].
 - [259] B. Feldstein, A. L. Fitzpatrick, and E. Katz, “Form Factor Dark Matter,” *JCAP* **1001** (2010) 020, [arXiv:0908.2991](#) [hep-ph].
 - [260] S. Chang, A. Pierce, and N. Weiner, “Momentum Dependent Dark Matter Scattering,” *JCAP* **1001** (2010) 006, [arXiv:0908.3192](#) [hep-ph].

- [261] N. Fornengo, P. Panci, and M. Regis, “Long-Range Forces in Direct Dark Matter Searches,” *Phys.Rev.* **D84** (2011) 115002, [arXiv:1108.4661 \[hep-ph\]](#).
- [262] **LUX Collaboration** Collaboration, D. Akerib *et al.*, “The Large Underground Xenon (LUX) Experiment,” *Nucl.Instrum.Meth.* **A704** (2013) 111–126, [arXiv:1211.3788 \[physics.ins-det\]](#).
- [263] **SuperCDMS Collaboration** Collaboration, P. Brink, “Conceptual Design for SuperCDMS SNOLAB,” *J.Low.Temp.Phys.* **167** (2012) 1093–1098.
- [264] S. Galli, F. Iocco, G. Bertone, and A. Melchiorri, “CMB constraints on Dark Matter models with large annihilation cross-section,” *Phys.Rev.* **D80** (2009) 023505, [arXiv:0905.0003 \[astro-ph.CO\]](#).
- [265] L. Lopez-Honorez, O. Mena, S. Palomares-Ruiz, and A. C. Vincent, “Constraints on dark matter annihilation from CMB observations before Planck,” [arXiv:1303.5094 \[astro-ph.CO\]](#).